

**BREAKDOWN OF LIESEGANG PRECIPITATION BANDS
IN A SIMPLIFIED FAST REACTION LIMIT
OF THE KELLER–RUBINOW MODEL**

ZYMANTAS DARBENAS AND MARCEL OLIVER*

ABSTRACT. We study solutions to the integral equation

$$\omega(x) = \Gamma - x^2 \int_0^1 K(\theta) H(\omega(x\theta)) d\theta$$

where $\Gamma > 0$, K is a weakly degenerate kernel satisfying, among other properties, $K(\theta) \sim k(1-\theta)^\sigma$ as $\theta \rightarrow 1$ for constants $k > 0$ and $\sigma \in (0, \log_2 3 - 1)$, H denotes the Heaviside function, and $x \in [0, \infty)$. This equation arises from a reaction-diffusion equation describing Liesegang precipitation band patterns under certain simplifying assumptions. We argue that the integral equation is an analytically tractable paradigm for the clustering of precipitation rings observed in the full model. This problem is nontrivial as the right hand side fails a Lipschitz condition so that classical contraction mapping arguments do not apply.

Our results are the following. Solutions to the integral equation, which initially feature a sequence of relatively open intervals on which ω is positive (“rings”) or negative (“gaps”) break down beyond a finite interval $[0, x^*]$ in one of two possible ways. Either the sequence of rings accumulates at x^* (“non-degenerate breakdown”) or the solution cannot be continued past one of its zeroes at all (“degenerate breakdown”). Moreover, we show that degenerate breakdown is possible within the class of kernels considered. Finally, we prove existence of generalized solutions which extend the integral equation past the point of breakdown.

1. INTRODUCTION

Reaction-diffusion equations with discontinuous hysteresis occur in a range of modeling problems [3, 18, 21, 26, 27]. We are particularly interested in non-ideal relays—two-valued operators where the output switches from the “off-state” 0 to the “on-state” 1 when the input crosses a threshold β , and switches back to zero only when the input drops below a lower threshold $\alpha < \beta$. There are different choices to define the behavior of the relay at the threshold. The relay may be restricted to binary values and jump when the threshold is reached or exceeded. Alternatively, the relay may be *completed*: when the threshold is reached but not exceeded, the relay may take fractional values which can change monotonically in time; when the input drops below the threshold without having crossed, the

Date: March 16, 2022.

2010 Mathematics Subject Classification. 34C55, 45G10.

Key words and phrases. Nonlinear integral equations, relay hysteresis, reaction-diffusion equations, Liesegang rings.

*Corresponding author, m.oliver@jacobs-university.de.

attained fractional value gets “frozen in”. See, e.g., [5] for a detailed description of different relay behaviors.

Rigorous mathematical results are of two types. For reaction-diffusion equations with completed relays, weak limit arguments lead to existence of solution [25, 2] but not necessarily their uniqueness and continuous dependence on the data. For reaction-diffusion equations with non-completed non-ideal relays, local well-posedness, including uniqueness and continuous dependence, holds true provided that a certain transversality condition on the data is satisfied. The solution can be continued in time for as long as the transversality condition remains satisfied [13, 12, 5]. We finally remark that for some types of spatially distributed hysteresis, variational approaches may be available [22].

In this paper, we study an explicit example of a reaction-diffusion equation with relay hysteresis which demonstrates that, in general, global-in-time solutions require the notion of a completed relay. Our example is motivated from the study of the fast reaction limit, introduced by Hillhorst *et al.* [15, 16], of the Keller and Rubinow model for Liesegang precipitation rings [17]. This limit model, which we will refer to as the *HHMO-model*, is a scalar reaction-diffusion equation driven by a point source which is constant in parabolic similarity variables with a reaction term modeled by a relay with a positive upper threshold and zero lower threshold. As a consequence, at a fixed location in space, the reaction, once switched on, can never switch off. The loci of reaction then form a spatial precipitation pattern.

Simple as it seems, an analysis of the HHMO-model faces the same type of difficulty as the analysis of other reaction-diffusion equations with relay hysteresis; in particular, the questions of global uniqueness and continuous dependence on the data remain open. Our aim here is to provide insight into the essential features of the distributed relay dynamics. We make use of a remarkable feature of the HHMO-model: it can be formally simplified to an equation, different but qualitatively similar to the actual HHMO-model, that is self-similar in parabolic similarity variables. This new model, which we shall refer to as the *simplified HHMO-model*, reduces to a single scalar integral equation, i.e., can be considered as a scalar dynamical system with memory. The simplified model is finally simple enough that a fairly complete explicit analysis is possible, which is the main contribution of this paper.

We prove that the binary precipitation pattern in the dynamics of the simplified HHMO-model must break down in finite space-time. Beyond the point of breakdown, it can only be continued as a generalized solution. We think of the behavior prior to breakdown as analogous to the well-posedness result for binary switching relays in the spirit of Gurevich *et al.* [12] and the behavior past the point of breakdown as generalized solutions in the sense of Visintin [25]. While these analogies are tentative and we make no claim that the simplified HHMO-model reflects the behavior of true Liesegang precipitation patterns, the study of this model offers a paradigm for the breakdown of binary patterns. In particular, it gives insight that breakdown can happen in two distinct ways. We believe that more general models—which may not share the symmetry which makes the explicit results of this paper possible—are capable of exhibiting the behaviors observed here, so that the results of this paper provide a lower bound on the complexity which must be

addressed when studying more general situations. We also offer a possible perspective for a reformulation of the problem that may lead to well-posedness past the point of breakdown.

To be specific, the simplified HHMO-model can be formulated as

$$\omega(x) = \Gamma - x^2 \int_0^1 K(\theta) H(\omega(x\theta)) d\theta, \quad (1)$$

where $\omega(x)$ is the excess reactant concentration at the source point, Γ is a positive constant, H denotes the Heaviside function, and K is a unimodal kernel, continuous on $[0, 1]$, continuously differentiable on $[0, 1)$, and twice continuously differentiable in the interior of this interval, with the following properties:

- (i) $K(\theta)$ is non-negative with $K(0) = K'(0) = 0$,
- (ii) $K(\theta) \sim k\sqrt{1-\theta}$ as $\theta \rightarrow 1$ for some $k > 0$,
- (iii) there exists $\theta^* \in (0, 1)$ such that $K''(\theta) > 0$ for $\theta \in (0, \theta^*)$ and $K''(\theta) < 0$ for $\theta \in (\theta^*, 1)$.

These properties imply, in particular, that $K > 0$ on $(0, 1)$ and $K(1) = 0$.

Clearly, at $x_0 = 0$, $\omega(x_0) = \Gamma > 0$ and there must be a point x_1 at which ω changes sign, i.e., where the concentration falls below the super-saturation threshold. Continuing, we may define a sequence x_i of loci where ω changes sign, so that (x_i, x_{i+1}) corresponds to a “ring” or “band” where precipitation occurs when i is even and to a precipitation gap when i is odd. Given the physical background of the problem, we might think that the x_i form an unbounded sequence, indicating that the entire domain is covered by a pattern of rings or gaps, or, if the sequence is finite, that the last ring or gap extends to infinity.

Our first result proves that this is not the case: The sequence x_i either has a finite accumulation point x^* or there is a finite index i such that ω cannot be extended past $x^* = x_i$ in the sense of equation (1). We call the former case non-degenerate, the latter degenerate.

Our second result demonstrates the existence of degenerate solutions to (1). To this end, we present the construction of a kernel where the solution cannot be continued past the first gap, i.e., where the point of breakdown is $x^* = x_2$.

To extend the solution past x^* , we introduce the concept of *extended solutions*, reflecting the concept of a completed relay in the spirit of [25] and also [16]. Extended solutions are pairs (ω, ρ) where $\omega \in C([0, \infty))$ and

$$\omega(x) = \Gamma - x^2 \int_0^1 K(\theta) \rho(x\theta) d\theta, \quad (2)$$

subject to the condition that ρ takes values from the Heaviside graph, i.e.,

$$\rho(y) \in H(\omega(y)) = \begin{cases} 0 & \text{if } \omega(y) < 0, \\ [0, 1] & \text{if } \omega(y) = 0, \\ 1 & \text{otherwise.} \end{cases} \quad (3)$$

As our third result, we prove existence of extended solutions. Extended solutions are unique under the condition that they are *regularly extended*, namely that ω remains identically zero on some right neighborhood $[x^*, b)$ past the point of breakdown.

The remainder of the paper is structured as follows. In Section 2, we recall some background on Liesegang rings and the fast reaction limit of the Keller–Rubinow model. In Section 3, we simplify the model to the scalar integral equation (1) and

present arguments and numerical evidence that the simplified model reflects the qualitative behavior of the full model. We then proceed to show, in Section 4, that the sequence of precipitation bands either terminates finitely or has a finite accumulation point. In Section 5, we provide a construction that shows that within the class of kernels considered, finite termination is possible. Section 6 discusses extended solutions in the sense of (2). We conclude with a brief discussion and outlook.

2. THE KELLER–RUBINOW MODEL IN THE FAST REACTION LIMIT

Liesegang precipitation bands are structured patterns in reaction-diffusion kinetics which emerge when, in a chain of two chemical reactions, the second reaction is triggered upon exceeding a supersaturation threshold and is maintained until the reactant concentration falls below a lower so-called saturation threshold. Within suitable parameter ranges, the second reaction will only ignite in restricted spatial regions. When the product of the final reaction precipitates, these regions may be visible as “Liesegang rings” or “Liesegang bands” in reference to German chemist Raphael Liesegang who described this phenomenon in 1896. For a review of the history and chemistry of Liesegang patterns, see [14, 24].

Keller and Rubinow [17] gave a quantitative model of Liesegang bands in terms of coupled reaction-diffusion equations, see [10, 11] for recent results and further references. We note that there is a competing description in terms of competitive growth of precipitation germs [23] which will not play any role in the following; see, e.g., [19] for a comparative discussion.

Our starting point is the fast reaction limit of the Keller–Rubinow model, where the first-stage reaction rate constant is taken to infinity and one of the first-stage reactant is assumed to be immobile. Hilhorst *et al.* [15, 16] proved that, in this limit, the first-stage reaction can be solved explicitly and contributes a point source of reactant to the second-stage process. Thus, only one scalar reaction-diffusion equation for the second-stage reactant concentration $u = u(x, t)$ remains. Formulated on the half-line, the fast reaction limit, which we shall refer to as the *full* HHMO-model, reads as follows:

$$u_t = u_{xx} + \frac{\alpha\beta}{2\sqrt{t}} \delta(x - \alpha\sqrt{t}) - p[x, t; u] u, \quad (4a)$$

$$u_x(0, t) = 0 \quad \text{for } t \geq 0, \quad (4b)$$

$$u(x, 0) = 0 \quad \text{for } x > 0, \quad (4c)$$

where α and β are positive constants and the precipitation function $p[x, t; u]$ is constrained by

$$p(x, t) \in \begin{cases} 0 & \text{if } \sup_{s \in [0, t]} u(x, s) < u^*, \\ [0, 1] & \text{if } \sup_{s \in [0, t]} u(x, s) = u^*, \\ 1 & \text{if } \sup_{s \in [0, t]} u(x, s) > u^*. \end{cases} \quad (4d)$$

In this expression, $u^* > 0$ is the super-saturation threshold, i.e., the ignition threshold for the second-stage reaction. For simplicity, the saturation threshold is taken to be zero. This means that once the reaction is ignited at some spatial location x , it will not ever be extinguished at x .

Hilhorst *et al.* [16] proved existence of weak solutions to (4); the question of uniqueness was left open. It is important to note that a weak solution is always

a tuple (u, p) where p is constrained, but not defined uniquely in terms of u , by (4d). The analytic difficulties lie in the fact that the onset of precipitation is a free boundary in the (x, t) -plane. Moreover, the precipitation term is discontinuous, so that most of the standard analytical tools are not applicable; in particular, estimates based on energy stability fail. In [6, 7], we are able to prove uniqueness for at least an initial short interval of time and derive a sufficient condition for uniqueness at later times; we conjecture that it is possible to obtain instances of non-uniqueness when the problem is considered with arbitrary smooth initial data or smooth additional forcing. One of the questions posed in [16] is the problem of proving that the precipitation function p takes only binary values.

Numerical evidence suggests that after an initial transient period in which a small number of rapidly shrinking rings is visible, the solution appears to precipitate on single grid points whose exact locations are unstable with respect to grid refinement. Results specifically for the HHMO-model are reported in Section 3 below; Duley *et al.* [10] report similar behavior also for the original Keller–Rubinow model. The main result of this paper is that we suggest a mechanism by which an actual breakdown of the ring structure in the Keller–Rubinow model occurs. It is made rigorous for a simplified version of the HHMO-model, introduced in the following, but displays features that are also seen in both of its parent models.

3. THE SIMPLIFIED HHMO-MODEL

In the following, we detail the connection between the full HHMO-model (4) and the integral equation (1). The key observation is that, when written in a suitable equivalent form, there are only two terms in the full model which do not possess a parabolic scaling symmetry. We cite a mixture of analytic and numerical evidence that suggest that these terms have a negligible impact on the long-time behavior of the solution: One of the neglected terms represents linear damping toward equilibrium. It is asymptotically subdominant relative to the precipitation term; moreover, its presence could only enhance relaxation to equilibrium. The other term is observed to be asymptotically negligible as the width of the precipitation rings decreases, hence its contribution vanishes as the point of breakdown is approached. Leaving only terms which scale parabolically self-similarly, one of the variables of integration in the Duhamel formula representation of the simplified model can be integrated out, leaving an expression of the form (1) with a complicated, yet explicit expression for the kernel K which is shown, using a mixture of analysis and numerical verification, to satisfy properties (i)–(iii).

Numerical evidence suggests that solutions to the full HHMO-model converge robustly to a steady state $\Phi(\eta)$ with respect to the parabolic similarity variable $\eta = x/s$ as $s = \sqrt{t} \rightarrow \infty$, see Figure 1 which is explained in detail further below. A proof of convergence to a steady state is difficult for much the same reasons that well-posedness is difficult, but [9] were able to prove a slightly weaker result: *assuming* that the HHMO-solution converges to a steady state $\Phi(\eta)$ at all, this

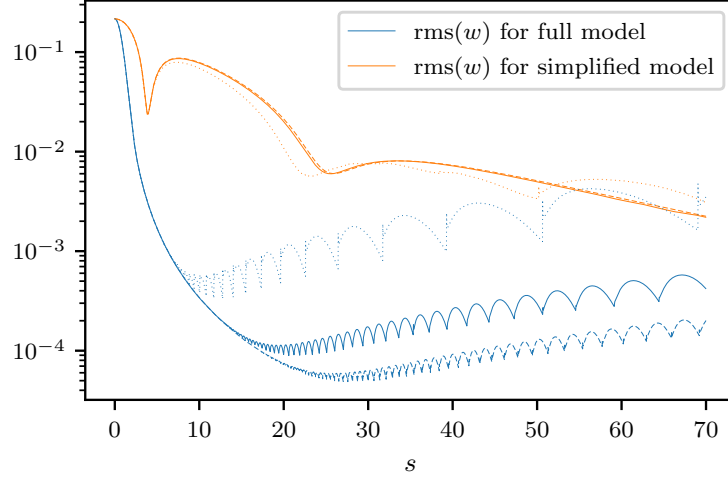


FIGURE 1. Numerical verification of the convergence of the full and the simplified HHMO-model to the self-similar profile Φ . Even though the transients are different, the difference field w converges to zero in both cases. Model parameters are $\alpha = \beta = 1$ and $u^* = 0.2$. The simulation shows that numerical artifacts at large times decrease with improved resolution, where $\Delta s = \Delta \eta = 10^{-2}$ (dotted lines), $\Delta s = \Delta \eta = 10^{-3}$ (dashed lines), and $\Delta s = \Delta \eta = 10^{-4}$ (solid lines). See text for a detailed discussion.

steady state must satisfy the differential equation

$$\Phi'' + \frac{\eta}{2} \Phi' + \frac{\alpha\beta}{2} \delta(\eta - \alpha) - \frac{\gamma}{\eta^2} H(\alpha - \eta) \Phi = 0, \quad (5a)$$

$$\Phi'(0) = 0, \quad (5b)$$

$$\Phi(\eta) \rightarrow 0 \quad \text{as } \eta \rightarrow \infty, \quad (5c)$$

$$\Phi(\alpha) = u^*. \quad (5d)$$

In this formulation, γ is an unknown constant. To determine γ uniquely, this second order system has an additional internal boundary condition (5d) which expresses that the reactant concentration in the HHMO-model converge to the critical value u^* at the source point which, in similarity coordinates, moves along the line $\eta = \alpha$.

There exists a unique solution (Φ, γ) to (5) with $\gamma > 0$ and Φ given by

$$\Phi(\eta) = \begin{cases} \frac{u^* \eta^\kappa M\left(\frac{\kappa}{2}, \kappa + \frac{1}{2}, -\frac{\eta^2}{4}\right)}{\alpha^\kappa M\left(\frac{\kappa}{2}, \kappa + \frac{1}{2}, -\frac{\alpha^2}{4}\right)} & \text{if } \eta < \alpha, \\ \frac{u^*}{\operatorname{erfc}\left(\frac{\alpha}{2}\right)} \operatorname{erfc}\left(\frac{\eta}{2}\right) & \text{if } \eta \geq \alpha, \end{cases} \quad (6)$$

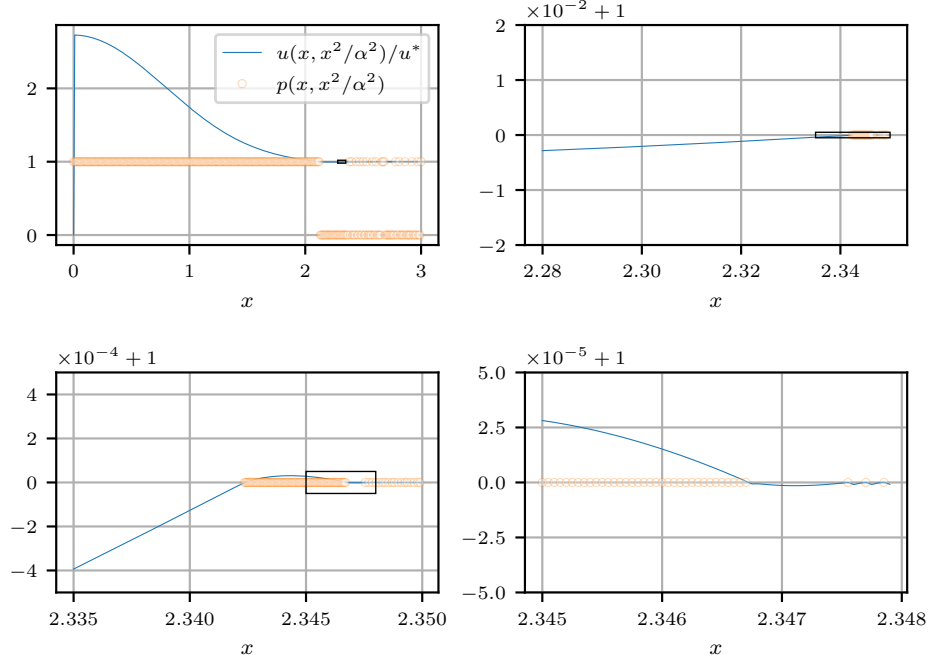


FIGURE 2. Relative concentration u/u^* and precipitation function p along the parabola $t = x^2/\alpha^2$ for the full HHMO-model. Each subsequent graph zooms into the boxed area of the previous. The simulation parameters are $\alpha = \beta = 1$, $u^* = 0.2$, $\Delta s = \Delta\eta = 5 \cdot 10^{-5}$. Note that the x -scale here coincides directly with similarity time $s = x/\alpha$ used in Figure 1.

where M is Kummer's confluent hypergeometric function [1], κ is a solution of the algebraic equation

$$u^* = u_\gamma^* \equiv \left(\frac{\kappa M\left(\frac{\kappa}{2} + 1, \kappa + \frac{1}{2}, -\frac{\alpha^2}{4}\right)}{\alpha M\left(\frac{\kappa}{2}, \kappa + \frac{1}{2}, -\frac{\alpha^2}{4}\right)} + \frac{\exp\left(-\frac{\alpha^2}{4}\right)}{\sqrt{\pi} \operatorname{erfc}\left(\frac{\alpha}{2}\right)} \right)^{-1} \frac{\alpha\beta}{2}, \quad (7)$$

and $\gamma = \kappa(\kappa - 1)$, subject to the solvability condition

$$u^* < u_0^*. \quad (8)$$

In x - t coordinates, the self-similar solution to (5) takes the form

$$\phi(x, t) = \Phi(x/\sqrt{t}). \quad (9)$$

Throughout this paper, we assume that α , β , and u^* satisfy the solvability condition (8), so that the self-similar solution ϕ exists. (For triples α , β , and u^* which violate the solvability condition, the corresponding weak solution precipitates in only a bounded region and the asymptotic state is easy to determine explicitly; for details, see [9].)

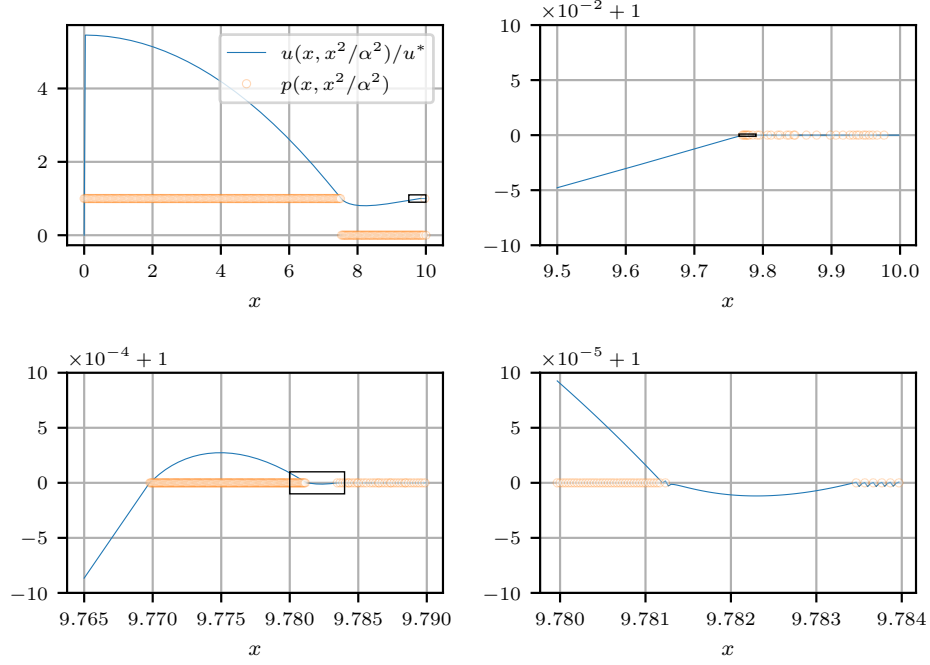


FIGURE 3. Relative concentration u/u^* and precipitation function p along the parabola $t = x^2/\alpha^2$ for the simplified HHMO-model. Each subsequent graph zooms into the boxed area of the previous. The simulation parameters are $\alpha = \beta = 1$, $u^* = 0.1$, $\Delta s = \Delta\eta = 3.33 \cdot 10^{-5}$. Note that the x -scale here coincides directly with similarity time $s = x/\alpha$ used in Figure 1.

We now write $w = u - \phi$ to denote the difference between the solution of the full HHMO-model (4) and the self-similar profile (9). Then w solves the equation

$$w_t - w_{xx} + pw = \left(\frac{\gamma}{x^2} H\left(\alpha - \frac{x}{\sqrt{t}}\right) - p \right) \phi\left(\frac{x}{\sqrt{t}}\right), \quad (10a)$$

$$w_x(0, t) = 0 \quad \text{for } t \geq 0, \quad (10b)$$

$$w(x, 0) = 0 \quad \text{for } x > 0. \quad (10c)$$

To pass to the simplified HHMO-model, we make two changes to this equation:

- (a) Precipitation is triggered on the condition that $u > u^*$ on the line $x^2 = \alpha^2 t$, and
- (b) the damping term pw in (10a) is neglected.

The simplified model then reads

$$w_t - w_{xx} = \left(\frac{\gamma}{x^2} - H\left(w\left(x, \frac{x^2}{\alpha^2}\right)\right) \right) H\left(\alpha - \frac{x}{\sqrt{t}}\right) \phi(x, t), \quad (11a)$$

$$w_x(0, t) = 0 \quad \text{for } t \geq 0, \quad (11b)$$

$$w(x, 0) = 0 \quad \text{for } x > 0. \quad (11c)$$

To illustrate the impact of these simplifications, we resort to numerical simulation. In the context of this problem, two general comments about numerical simulation are necessary.

First, we are looking at the long-time behavior of the solution where breakdown has already occurred early in the simulation. For lack of a clear alternative, numerical schemes are constructed under the assumption of a binary precipitation function. Thus, we cannot expect pointwise convergence of the precipitation function; convergence of the numerical precipitation function to the precipitation function of a weak solution in the sense of [16] can at best take place in the weak-* topology. The concentration, on the other hand, may converge point-wise. High-order convergence cannot be expected in this setting so that we limit ourselves to the lowest order finite difference approximations.

Second, the asymptotic profile is stationary in *similarity* variables, but a spatial grid cell of constant size in similarity variables maps to a cell in physical space whose size increases in time. This leaves fundamentally two options:

- (i) Compute on a fixed grid in physical space and accept that the essential part of the solution will run out of the computational domain in a finite time.
- (ii) Compute on a fixed grid in similarity variables and accept that the smallest unit of precipitation that can be represented by the scheme will get coarser as time goes on, leading to spurious oscillations with increasing amplitude at late times.

It is conceivable that an h - p -adaptive method on an essentially infinite domain in physical space could break this dichotomy, but would also raise the issue of how much such a complex scheme can be trusted, and how to adapt it to the essentially non-smooth nature of this problem. For these reasons, we choose not to take this route but rather accept that accuracy is lost as time progresses. The time of validity can be extended by choosing a finer spatial grid in similarity variables, or choosing a bigger domain in physical space. For any given grid, however, the time of validity is finite.

For our code, we have chosen a finite difference scheme formulated in similarity variables $\eta = x/\sqrt{t}$ and $s = \sqrt{t}$; it is detailed in Appendix B. The advantage is that it makes the identification of the limit profile particularly easy; the drawback is that it requires a transport scheme for the precipitation function, making the code just slightly longer than a direct solve in physical variables.

Figure 1 demonstrates that both the full HHMO-model and the simplified model converge to the asymptotic profile Φ , i.e., $\|w(t)\| \rightarrow 0$ as $t \rightarrow \infty$. As expected, due to the lack of the linear damping term pw , the simplified model takes longer to equilibrate, but the asymptotics remain unchanged. We note that the loss of accuracy with time, described above, is clearly visible. Increasing the numerical resolution moves the point of visible onset of numerical error to larger times, but the behavior of the scheme is fundamentally non-uniform in time.

Figures 2 and 3 show details of the initial transient of the full and the simplified model, respectively. We see that even though the transients are quantitatively different, the two models have the same qualitative features: The amplitude of the variation of concentration about the threshold concentration at the source point decreases extremely rapidly, as does the width of the precipitation rings and gaps. In both simulations, we were able to clearly resolve two precipitation rings and

two gaps, where the last gap is only visible by zooming in about five orders of magnitude. We cannot determine whether there is a third distinct ring; simulating this numerically would require at least one order of magnitude more resolution in space, due to the additional timestepping at least two orders of magnitude more in computational expense. In the following, we prove, for the simplified model, that the ring structure must break down within a finite interval; the simulations suggest that this interval is not particularly large.

We have also observed that most of the quantitative change comes from simplification (b). Implementing simplification (a) without simplification (b) yields a solution that is visually indistinguishable from the solution to the full model.

Note that simplification (a) implies that there is no precipitation below the line $x^2 = \alpha^2 t$, even when $u > u^*$. The advantage of this simplification is that onset of precipitation now ceases to be a free boundary problem and follows parabolic scaling. A motivation for the validity of this simplification comes from the following fact: it is proved in [9] that *if* the solution to the full HHMO-model converges to a parabolically self-similar profile as $t \rightarrow \infty$, then the contribution to the HHMO-dynamics from precipitation below the parabola $\alpha^2 t = x^2$ is asymptotically negligible.

Simplification (b) is justified by the numerical observation that the equation without the damping term pw already converges to the same profile, so that an additional linear damping toward the equilibrium will not make a qualitative difference. Moreover, assuming that the HHMO-solution converges to equilibrium, pw becomes asymptotically small while the right hand side of (10a) remains an order-one quantity. It is very difficult, however, to estimate the quantitative effect of (a) and (b) due to the discontinuous reaction term and the free boundary of onset of precipitation, so that a rigorous justification of these two steps remains open.

To proceed, we extend the simplified HHMO-model (11) to the entire real line by even reflection and abbreviate

$$\rho(x) = \frac{\gamma}{x^2} - H\left(w\left(x, \frac{x^2}{\alpha^2}\right)\right). \quad (12)$$

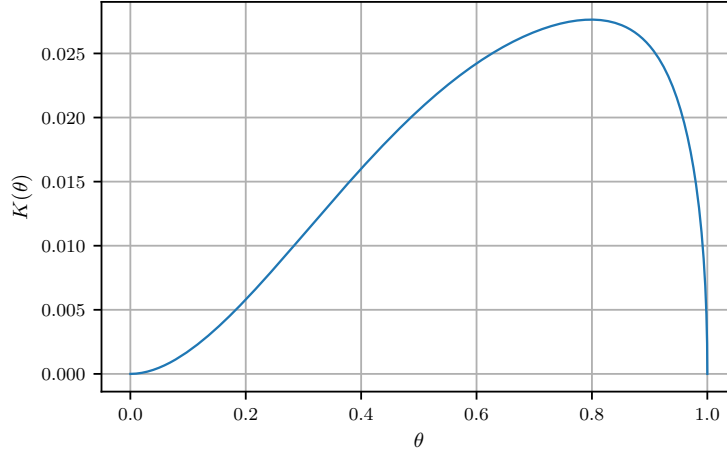
Proceeding formally, we apply the Duhamel principle—a detailed justification of the Duhamel principle in context of weak solutions is given in [6]—then change the order of integration and implement the change of variables $s = y^2/\zeta^2$, so that

$$\begin{aligned} w(x, t) &= \int_{-\alpha\sqrt{t}}^{\alpha\sqrt{t}} \int_{y^2/\alpha^2}^t \Theta(x - y, t - s) \phi(y, s) ds \rho(y) dy \\ &= 2 \int_{-\alpha\sqrt{t}}^{\alpha\sqrt{t}} \int_{|y|/\sqrt{t}}^{\alpha} \Theta(x - y, t - y^2/\zeta^2) \frac{\Phi(\zeta)}{\zeta^3} d\zeta \rho(y) y^2 dy \end{aligned} \quad (13)$$

where Θ is the standard heat kernel

$$\Theta(x, t) = \begin{cases} \frac{1}{\sqrt{4\pi t}} e^{-\frac{x^2}{4t}} & \text{if } t > 0, \\ 0 & \text{if } t \leq 0. \end{cases} \quad (14)$$

We are specifically interested in the solution on the parabola $x^2 = \alpha^2 t$. For notational convenience, we assume in the following that x is nonnegative; solutions for negative x are obtained by even reflection. Then, setting $\omega(x) = w(x, x^2/\alpha^2)$

FIGURE 4. Plot of the kernel $K(\theta)$ for $\alpha = \beta = 1$ and $u^* = 0.15$.

and inserting the fundamental solution of the heat equation explicitly, we find

$$\begin{aligned}
 \omega(x) &= \frac{1}{\sqrt{\pi}} \int_{-x}^x \int_{\alpha|y|/x}^{\alpha} \frac{1}{\sqrt{\frac{x^2}{\alpha^2} - \frac{y^2}{\zeta^2}}} \exp\left(-\frac{(x-y)^2}{4\left(\frac{x^2}{\alpha^2} - \frac{y^2}{\zeta^2}\right)}\right) \frac{\Phi(\zeta)}{\zeta^3} d\zeta \rho(y) y^2 dy \\
 &= \frac{1}{x} \int_{-x}^x G\left(\frac{y}{x}\right) \rho(y) y^2 dy \\
 &= x^2 \int_{-1}^1 G(\theta) \rho(x\theta) \theta^2 d\theta, \tag{15}
 \end{aligned}$$

where

$$G(\theta) = \frac{\alpha}{\sqrt{\pi}} \int_{\alpha|\theta|}^{\alpha} \frac{1}{\sqrt{\zeta^2 - \alpha^2 \theta^2}} \exp\left(-\frac{\zeta^2 \alpha^2 (1-\theta)^2}{4(\zeta^2 - \alpha^2 \theta^2)}\right) \frac{\Phi(\zeta)}{\zeta^2} d\zeta. \tag{16}$$

Inserting the explicit expression for ρ into (15) and noting that ω is extended to negative arguments by even reflection, we obtain

$$\omega(x) = \Gamma - x^2 \int_0^1 K(\theta) H(\omega(x\theta)) d\theta \tag{17}$$

with

$$\Gamma = \gamma \int_{-1}^1 G(\theta) d\theta \tag{18}$$

and

$$K(\theta) = \theta^2 (G(\theta) + G(-\theta)). \tag{19}$$

A graph of the kernel K is shown in Figure 4. In Appendix A, we give a combination of analytic and numerical evidence showing that this kernel satisfies properties (i)–(iii) stated in the introduction.

We conclude that the simplified HHMO-model implies an integral equation of the form (1). Vice versa, given a solution ω to (17), we can reconstruct a solution

to the PDE-formulation of the simplified HHMO-model. Indeed, setting

$$W(x, t) = \int_0^t \int_{-\alpha\sqrt{s}}^{\alpha\sqrt{s}} \Theta(x - y, t - s) \left(\frac{\gamma}{y^2} - H(\omega(y)) \right) \phi(y, s) dy ds, \quad (20)$$

we can repeat the calculation leading to (15), which proves that $W(x, \alpha^{-2}x^2) = \omega(x)$. Thus, W solves (13) so that it provides a mild solution to (11).

4. NON-DEGENERATE BREAKDOWN OF PRECIPITATION BANDS

In this section, we investigate the structure of solutions to the integral equation (1) for kernels K which satisfy assumptions (i)–(iii). Specifically, we seek solutions ω defined on a half-open interval $[0, x^*)$ or on $[0, \infty)$ which change sign at isolated points x_i for $i = 1, 2, \dots$, ordered in increasing sequence. Setting $x_0 = 0$ and noting that precipitation must occur in a neighborhood of the origin if it sets in at all, the precipitation bands are the intervals (x_i, x_{i+1}) for even integers $i \geq 0$. Hence,

$$H(\omega(z)) = \sum_{i \text{ even}} \mathbb{I}_{[x_i, x_{i+1}]}(z), \quad (21)$$

where we write \mathbb{I}_A to denote the indicator function of a set A . Thus, the one-dimensional precipitation equation (1) takes the form

$$\begin{aligned} \omega(x) &= \Gamma - x^2 \sum_{\substack{i \text{ even} \\ x_i < x}} \int_{x_i/x}^{\min\{x_{i+1}/x, 1\}} K(\theta) d\theta \\ &= \Gamma - \sum_{x_i < x} (-1)^i \rho_i(x) \end{aligned} \quad (22)$$

with

$$\rho_i(x) = x^2 \int_{x_i/x}^1 K(\theta) d\theta. \quad (23)$$

For $x \geq x_{n-1}$, we also define the partial sums

$$\omega_n(x) = \Gamma - \sum_{i=0}^{n-1} (-1)^i \rho_i(x). \quad (24)$$

Thus, $\omega_n(x) = \omega(x)$ for $x \in [x_{n-1}, x_n]$.

With this notation in place, we are able to define the notion of degenerate solutions.

Definition 1. *A solution ω to (1) is degenerate if (22) holds up to some finite $x_i \equiv x^*$ and it is not possible to apply this formula on $[x^*, x^* + \varepsilon)$ for any $\varepsilon > 0$; it is non-degenerate if ω possesses a finite or infinite sequence of isolated zeros $\{x_i\}$ and the solution can be continued in the sense of (22) to some right neighborhood of any of its zeros.*

In the remainder of this section, we characterize non-degenerate solutions. We cannot exclude that a solution is degenerate, i.e., that it cannot be continued at all beyond an isolated root; in fact, Section 5 shows that kernels with degenerate solutions exist. We note that a degenerate solution provides an extreme scenario of a breakdown in which the solution reaches equilibrium in finite time. Thus, the main result of this section, Theorem 4 below, can be understood as saying that even when the solution is non-degenerate, it still fails to exist outside of a bounded interval.

Lemma 2. *Suppose $K \in C([0, 1])$ is non-negative, strictly positive somewhere, and $K(\theta) = o(\theta)$ as $\theta \rightarrow 0$. Then a non-degenerate solution to (1) has an infinite number of precipitation rings.*

Proof. A non-degenerate solution, by definition, is a solution that can be extended to the right in some neighborhood of any of its zeros. Now suppose there is a largest zero x_n . Then ω is well-defined and equals ω_{n+1} on $[x_n, \infty)$. Now let $x > x_n$ and consider the limit $x \rightarrow \infty$. When n is even, since $\rho_{i+1}(x) < \rho_i(x)$,

$$0 < \omega(x) < \Gamma - \rho_n(x) \rightarrow -\infty, \quad (25)$$

a contradiction. When n is odd,

$$\begin{aligned} 0 > \omega(x) &> \Gamma - x^2 \int_0^{x_n/x} K(\theta) d\theta \\ &> \Gamma - x^2 \sup_{\theta \in [0, x_n/x]} \frac{K(\theta)}{\theta} \int_0^{x_n/x} \theta d\theta \\ &= \Gamma - \frac{1}{2} x_n^2 \sup_{\theta \in [0, x_n/x]} \frac{K(\theta)}{\theta} \rightarrow \Gamma > 0, \end{aligned} \quad (26)$$

once again a contradiction. \square

Lemma 3. *Suppose $K \in C([0, 1]) \cap C^1([0, 1])$ with $K(1) = 0$ and $K'(\theta) \rightarrow -\infty$ as $\theta \rightarrow 1$. Let ω be a non-degenerate solution to (1) with an infinite number of precipitation rings. Then $x_{2n}/x_{2n+1} \rightarrow 1$ as $n \rightarrow \infty$. Moreover, $x_{2n+1} - x_{2n}$, the width of the n th precipitation ring, converges to zero.*

Proof. When the sequence $\{x_i\}$ is bounded, the claim is obvious. Thus, assume that this sequence is unbounded. Since K' is negative on $(1 - \varepsilon, 1)$ for sufficiently small $\varepsilon > 0$, K is positive on this interval. As in the proof of Lemma 2,

$$0 \equiv \omega(x_{2n+1}) < \Gamma - \rho_{2n}(x_{2n+1}) = \Gamma - x_{2n+1}^2 \int_{x_{2n}/x_{2n+1}}^1 K(\theta) d\theta. \quad (27)$$

We can directly conclude that $x_{2n}/x_{2n+1} \rightarrow 1$ as $n \rightarrow \infty$. Further, noting that $K(1) = 0$ and using the fundamental theorem of calculus, we obtain

$$\begin{aligned} \Gamma &> x_{2n+1}^2 \int_{x_{2n}/x_{2n+1}}^1 (K(\theta) - K(1)) d\theta \\ &= -x_{2n+1}^2 \int_{x_{2n}/x_{2n+1}}^1 \int_{\theta}^1 K'(\zeta) d\zeta d\theta \\ &= -x_{2n+1}^2 \int_{x_{2n}/x_{2n+1}}^1 K'(\zeta) \int_{x_{2n}/x_{2n+1}}^{\zeta} d\theta d\zeta \\ &= -\frac{1}{2} K'(\zeta_n) (x_{2n+1} - x_{2n})^2 \end{aligned} \quad (28)$$

where, by the mean value theorem of integration, the last equality holds for some $\zeta_n \in [x_{2n}/x_{2n+1}, 1]$. Since $\zeta_n \rightarrow 1$, we conclude that $x_{2n+1} - x_{2n} \rightarrow 0$ as $n \rightarrow \infty$. \square

Theorem 4. *Suppose $K \in C([0, 1])$, differentiable with absolutely continuous first derivative on $[0, z]$ for every $z \in (0, 1)$, and unimodal, i.e., there exists $\theta^* \in (0, 1)$ such that $K''(\theta) > 0$ for $\theta \in (0, \theta^*)$ and $K''(\theta) < 0$ for $\theta \in (\theta^*, 1)$, and that $K(\theta) \sim k(1 - \theta)^\sigma$ for some $k > 0$ and $\sigma \in (0, \log_2 3 - 1)$ as $\theta \rightarrow 1$. Further,*

assume that equation (1) has a non-degenerate solution ω with an infinite number of precipitation rings. Then its zeros have a finite accumulation point.

Proof. We begin by recalling the second order mean value theorem, which states that for a twice continuously differentiable function f and nodes $a < b < c$ there exists $y \in [a, c]$ such that

$$\frac{f(c) - f(b)}{c - b} - \frac{f(b) - f(a)}{b - a} = \frac{c - a}{2} f''(y). \quad (29)$$

We apply this result to the partial sum function ω_n with $a = x_n$, $b = x_{n+1}$, and $c = x \in (x_{n+1}, x_{n+2}]$. We note that $\omega_n(x_n) = 0$. Further, subtracting (24) from (22), we obtain, for $x \in [x_{n+1}, x_{n+2}]$, that

$$\omega_n(x) = \omega(x) + (-1)^n (\rho_n(x) - \rho_{n+1}(x)) \quad (30)$$

so that, in particular, $\omega_n(x_{n+1}) = (-1)^n \rho_n(x_{n+1})$. Equation (29) then reads

$$\frac{\omega(x) + (-1)^n (\rho_n(x) - \rho_{n+1}(x) - \rho_n(x_{n+1}))}{x - x_{n+1}} - \frac{(-1)^n \rho_n(x_{n+1})}{x_{n+1} - x_n} = \frac{x - x_n}{2} \omega_n''(y) \quad (31)$$

for some $y \in [x_n, x]$.

To estimate the right hand expression, we compute

$$\omega_n''(y) = \sum_{i=0}^{n-1} (-1)^i F\left(\frac{x_i}{y}\right) \equiv \sum_{i=0}^{n-1} (-1)^i f_i \quad (32)$$

where

$$F(z) = z^2 K'(z) - 2z K(z) - 2 \int_z^1 K(\theta) d\theta. \quad (33)$$

By direct computation, $F'(z) = z^2 K''(z)$. Since K is unimodal, this implies that F has an isolated maximum on $[0, 1]$.

Now suppose that $x \in (x_{n+1}, x_{n+2})$. We consider two separate cases. When n is even, for every $y \geq x_{n-1}$ there exists a unique odd index ℓ such that the sequence of f_i is strictly increasing for $i = 1, \dots, \ell - 1$ and is strictly decreasing for $i = \ell + 1, \dots, n - 1$. Hence,

$$\begin{aligned} \omega_n''(y) &= f_0 + (-f_1 + f_2) + \dots - f_\ell + (f_{\ell+1} - f_{\ell+2}) + \dots + (f_{n-2} - f_{n-1}) \\ &> f_0 - f_\ell \geq F(0) - \max_{z \in [0,1]} F(z) \equiv -M, \end{aligned} \quad (34)$$

where M is a strictly positive constant. Further, $\omega(x) < 0$. Inserting these two estimates into (31), we obtain

$$\frac{\rho_n(x) - \rho_{n+1}(x) - \rho_n(x_{n+1})}{x - x_{n+1}} - \frac{\rho_n(x_{n+1})}{x_{n+1} - x_n} > -\frac{x - x_n}{2} M. \quad (35)$$

When n is odd, for every $y \geq x_{n-1}$ there exists a unique even index ℓ such that the sequence of f_i is strictly increasing for $i = 0, \dots, \ell - 1$ and is strictly decreasing for $i = \ell + 1, \dots, n - 1$. Hence,

$$\begin{aligned} \omega_n''(y) &= (f_0 - f_1) + \dots + f_\ell + (-f_{\ell+1} + f_{\ell+2}) + \dots + (-f_{n-2} + f_{n-1}) \\ &< f_\ell \leq \max_{z \in [0,1]} F(z) = M + F(0) < M \end{aligned} \quad (36)$$

Further, $\omega(x) > 0$. As before, inserting these two estimates into (31), we obtain

$$-\frac{\rho_n(x) - \rho_{n+1}(x) - \rho_n(x_{n+1})}{x - x_{n+1}} + \frac{\rho_n(x_{n+1})}{x_{n+1} - x_n} < \frac{x - x_n}{2} M. \quad (37)$$

Thus, we again obtain an estimate of exactly the form (35) and we do not need to further distinguish between n even or odd.

To proceed, we define

$$R(\theta) = \frac{\int_{\theta}^1 K(\zeta) d\zeta}{k \int_{\theta}^1 (1 - \zeta)^{\sigma} d\zeta} \quad (38)$$

so that, by assumption, $R(\theta) \rightarrow 1$ as $\theta \rightarrow 1$. Further,

$$\rho_i(x) = \frac{k}{1 + \sigma} x^2 \left(1 - \frac{x_i}{x}\right)^{1+\sigma} R\left(\frac{x_i}{x}\right). \quad (39)$$

Changing variables to

$$d_n = x_{n+1} - x_n, \quad r_n = \frac{x_n}{x_{n+1}}, \quad \text{and} \quad q = \frac{x - x_{n+1}}{d_n}, \quad (40)$$

we write inequality (35) in the form

$$G(q) > -S_0(r_n, q) + S_1(r_n, q) (1 + q)^{1+\sigma} - S_2(r_n, q) q^{1+\sigma} - S_3(r_n, q) (q + 1) \quad (41)$$

where

$$S_0(r, q) = -q(q + 1) \left(\frac{1 - r}{1 + (1 - r)q}\right)^{1-\sigma} \frac{M(1 + \sigma)}{2k}, \quad (42a)$$

$$S_1(r, q) = 1 - R\left(\frac{r}{1 + (1 - r)q}\right), \quad (42b)$$

$$S_2(r, q) = 1 - R\left(\frac{1}{1 + (1 - r)q}\right), \quad (42c)$$

$$S_3(r, q) = 1 - \left(\frac{1}{1 + (1 - r)q}\right)^{1-\sigma} R(r), \quad (42d)$$

and

$$G(q) = (1 + q)^{1+\sigma} - q^{1+\sigma} - q - 1. \quad (42e)$$

Observe that $G(0) = 0$, $G'(0) > 0$, $G''(q) < 0$ for all $q > 0$, and $G(1) = 2^{1+\sigma} - 3 < 0$. Hence, there is a unique root $q^* \in (0, 1)$ such that $G(q) < 0$ for all $q > q^*$. Now fix $\varepsilon > 0$, define

$$q_n = \frac{x_{n+2} - x_{n+1}}{x_{n+1} - x_n}, \quad (43)$$

and consider any even index j for which $q_j > q^* + \varepsilon$. Since (41) was derived under the assumption $x \in (x_{j+1}, x_{j+2})$, or equivalently $q \in (0, q_j)$, this inequality must hold for each tuple $(r_j, q^* + \varepsilon)$. Now if there were an infinite set of indices for which $q_j > q^* + \varepsilon$, we could pass to the limit $j \rightarrow \infty$ on the subsequence of such indices. Since $K''(\theta) < 0$ for $\theta \in (\theta^*, 1)$ and $K(\theta) \sim k(1 - \theta)^{\sigma}$ as $\theta \rightarrow 1$, Lemma 3 is applicable and implies that $r_{2k} = x_{2k}/x_{2k+1} \rightarrow 1$. As for any fixed q , each of the $S_i(r, q)$ converges to zero as $r \rightarrow 1$, we arrive at the contradiction $G(q^* + \varepsilon) > 0$. Hence,

$$\limsup_{\substack{k \rightarrow \infty \\ k \text{ even}}} q_k \leq q^* < 1. \quad (44)$$

To extend this result to odd n , we note that

$$r_{n+1} = \frac{x_{n+1}}{x_{n+2}} = \frac{1}{1 + q_n(1 - r_n)} = \frac{(1 - r_n)(1 - r_n q_n)}{1 + q_n(1 - r_n)} + r_n > r_n \quad (45)$$

for all large enough even n . This implies an even stricter bound on the right hand side of (41) when n is replaced by $n + 1$, so that (44) holds on the subsequence of odd integers as well.

Altogether, this proves that the sequence of internodal distances $d_n = x_{n+1} - x_n$ is geometric, thus the x_n have a finite limit. \square

Remark 5. Note that in the proof of Theorem 4, we only need a result which is weaker than the statement of Lemma 3, namely that $r_n \rightarrow 1$ for even n going to infinity

Remark 6. Note that the argument yields an explicit upper bound for q_n , namely

$$\limsup_{n \rightarrow \infty} q_n \leq q^* < 1 \quad (46)$$

where, as in the proof, q^* is the unique positive root of G , which is defined in (42e).

Remark 7. It is possible to relax the unimodality condition in the statement of Theorem 4. In fact, it suffices that $\lim_{\theta \nearrow 1} K''(\theta) = -\infty$. Indeed, assume that K'' is defined on U_K . Take any $\theta^* \in (0, 1)$ such that $K'' < 0$ on $[\theta^*, 1) \cap U_K$. Changing variables in (24), we obtain

$$\omega_n(x) = \Gamma - x \int_0^x \mathbb{I}_{[0, x_n]}(y) K\left(\frac{y}{x}\right) H(\omega(y)) dy. \quad (47)$$

When n is even and $x \in (x_{n+1}, x_{n+2})$, the singularity of K' and K'' at $\theta = 1$ is separated from the domain of integration. We can therefore differentiate under the integral, so that

$$\omega'_n(x) = \frac{1}{x} \int_0^x \mathbb{I}_{[0, x_n]}(y) K'\left(\frac{y}{x}\right) y H(\omega(y)) dy - \int_0^x \mathbb{I}_{[0, x_n]}(y) K\left(\frac{y}{x}\right) H(\omega(y)) dy \quad (48)$$

and

$$\begin{aligned} \omega''_n(x) &= -\frac{1}{x^3} \int_0^x \mathbb{I}_{[0, x_n]}(y) K''\left(\frac{y}{x}\right) y^2 H(\omega(y)) dy \\ &= -\int_0^1 \mathbb{I}_{[0, x_n/x]}(\theta) K''(\theta) \theta^2 H(\omega(\theta x)) d\theta \\ &\geq -\int_0^{\theta^*} |K''(\theta)| \theta^2 d\theta > -\infty. \end{aligned} \quad (49)$$

When n is odd, then for every $x \in (x_{n+1}, x_{n+2})$ there is an even index ℓ such that $x_{\ell-1} < x\theta^* \leq x_{\ell+1}$ (with the provision that $x_{-1} = 0$), and

$$\omega''_n(x) = -x^{-3} \int_0^{x_{\ell-1}} K''\left(\frac{y}{x}\right) y^2 H(\omega(y)) dy + \sum_{i=\ell}^{n-1} (-1)^i F\left(\frac{x_i}{x}\right), \quad (50)$$

where F is as in (33). As in the proof of the theorem, $F'(z) = z^2 K''(z) < 0$ on $[\theta^*, 1)$ so that $M^* = \max_{z \in [0, 1]} F(z)$ is finite and

$$\sum_{i=\ell}^{n-1} (-1)^i F\left(\frac{x_i}{x}\right) \leq F\left(\frac{x_\ell}{x}\right) \leq M^*. \quad (51)$$

Therefore,

$$\omega_n''(x) \leq - \int_0^{x_\ell/x} K''(\theta) \theta^2 d\theta + M^* \leq \int_0^{\theta^*} |K''(\theta)| \theta^2 d\theta + M^* < \infty. \quad (52)$$

Hence, (35) and (37) continue to hold and the remainder of the proof proceeds as before.

Corollary 8. *Suppose that K satisfies conditions (i)–(iii) stated in the introduction. Then there exists $x^* < \infty$ so that the maximal interval of existence of a precipitation ring pattern in the sense of (22) is $[0, x^*]$.*

Proof. When the solution is degenerate, then such x^* exists by definition. Otherwise, property (i) and the positivity of the kernel on $(0, 1)$ imply that Lemma 2 is applicable, i.e., there exist an infinite number of precipitation rings. Then, due to properties (ii) and (iii), Theorem 4 applies and asserts the existence of a finite accumulation point x^* of the ring pattern. \square

5. EXISTENCE OF DEGENERATE SOLUTIONS

In this section, we show that degenerate solutions exist. These are solutions to (1) which cannot be continued past a finite number of zeros. While we cannot settle this question for the concrete kernel introduced in Section 3, we construct a kernel K such that the solution cannot be continued in the sense of (1) past x_2 , the end point of the first precipitation gap.

Theorem 9. *There exist a non-negative kernel $K \in C([0, 1])$ and a constant Γ such that the solution of the integral equation (1) is degenerate. Moreover, K is differentiable at $\theta = 0$ and satisfies conditions (i) and (ii).*

Remark 10. The proof starts from a kernel template which is then modified on a subinterval $[0, r)$ to produce a kernel K with the desired properties. When the kernel template is $C^1([0, 1])$ and $C^2((0, 1))$, the resulting kernel K will inherit these properties except possibly at the gluing point $\theta = r$ where continuity of the first derivative is not enforced. This is a matter of convenience, not of principle: The existence of degenerate solutions does not hinge on the existence of a jump discontinuity for K' . Straightforward, yet technical modifications of the gluing construction employed in the proof will yield a kernel producing degenerate solutions within the same class of kernels to which Theorem 4, in the sense of Remark 7, applies.

Remark 11. In Section 3, we derived a concrete kernel by simplifying the HHMO-model. In that setting, there exists an integrable function G such that $K(\theta) = \theta^2 G(\theta)$ and

$$\Gamma = \int_0^1 G(\theta) d\theta. \quad (53)$$

In the proof of the theorem, we preserve this relationship, i.e., the constant Γ here will also satisfy (53).

Proof. Take any continuous template kernel $G_* : [0, 1] \rightarrow \mathbb{R}_+$ with $G_*(\theta) \sim k\sqrt{1-\theta}$ as $\theta \rightarrow 1$ for some positive constant k . Set $K_*(\theta) = \theta^2 G_*(\theta)$ and

$$\Gamma = \int_0^1 G_*(\theta) d\theta. \quad (54)$$

Then $K_*(0) = 0$ and

$$K'_*(0) = \lim_{\theta \searrow 0} \frac{K_*(\theta)}{\theta} = \lim_{\theta \searrow 0} \theta G_*(\theta) = 0. \quad (55)$$

Now consider the solution to (1) with template kernel K_* in place of K . As in the proof of Lemma 2, the solution must have at least two zeros x_1 and x_2 . Let

$$\omega_*(x) = \begin{cases} \Gamma - x^2 \int_0^1 K_*(\theta) d\theta & \text{if } x < x_1, \\ \Gamma - x^2 \int_0^{x_1/x} K_*(\theta) d\theta & \text{otherwise.} \end{cases} \quad (56)$$

In the following we assume, for simplicity, that $\omega'_*(x_2) > 0$. This is true for generic template kernels G_* , thus suffices for the construction. However, it is also possible to modify the procedure to come to the same conclusion then $\omega'_*(x_2) = 0$; for details, see [6].

Note that ω_* is continuously differentiable on $[0, x_2]$, so $\omega'_*(x_2 - \varepsilon) > 0$ for all $\varepsilon > 0$ small enough. For each such small ε , set

$$\omega_\varepsilon(x) = \begin{cases} \omega_*(x) & \text{for } x \in [0, x_2 - \varepsilon], \\ \frac{1}{2} x^2 \int_{\frac{x_2 + \varepsilon}{x}}^1 K_*(\theta) d\theta & \text{for } x \in [x_2 + \varepsilon, z_\varepsilon], \end{cases} \quad (57)$$

where $z_\varepsilon \in (x_2 + \varepsilon, x_2 + 2\varepsilon]$ is chosen such that $\omega_\varepsilon(z_\varepsilon) \leq \Gamma/2$. (This is always possible because $\omega_\varepsilon(x_2 + \varepsilon) = 0$ and the second case expression in (57) is continuous, so we can take z_ε such that $\omega_\varepsilon(z_\varepsilon) = \Gamma/2$ if such solution exists on $(x_2 + \varepsilon, x_2 + 2\varepsilon]$, otherwise we take $z_\varepsilon = x_2 + 2\varepsilon$.) We now fill the gap in the definition of ω_ε such that

- (a) $\omega_\varepsilon : [0, x_2 + 2\varepsilon] \rightarrow \mathbb{R}$ is continuously differentiable,
- (b) ω_ε is increasing on $[x_2 - \varepsilon, x_2 + 2\varepsilon]$,
- (c) $\omega_\varepsilon < \Gamma$ on $[x_2 - \varepsilon, x_2 + 2\varepsilon]$.

Observe that $\omega_\varepsilon(x_2 + \varepsilon) = 0$. Moreover, due to the positivity of K_* , ω_ε is positive and strictly increasing on the interval $(x_2 + \varepsilon, z_\varepsilon]$, and

$$\omega'_\varepsilon(x) = x \int_{\frac{x_2 + \varepsilon}{x}}^1 K_*(\theta) d\theta + \frac{1}{2} (x_2 + \varepsilon) K_*\left(\frac{x_2 + \varepsilon}{x}\right). \quad (58)$$

Hence, $\omega'_\varepsilon(x_2 + \varepsilon) = 0$.

We now define a new kernel $K_\varepsilon : [x_1/(x_2 + 2\varepsilon), 1] \rightarrow \mathbb{R}_+$ via

$$K_\varepsilon(\theta) = \frac{\omega'_\varepsilon(x_1/\theta)}{x_1} - 2\theta \frac{\omega_\varepsilon(x_1/\theta) - \Gamma}{x_1^2} \quad (59)$$

and set $G_\varepsilon(\theta) = K_\varepsilon(\theta)/\theta^2$. Due to (b) and (c) above, K_ε is positive on its interval of definition. Moreover, for $x \in (x_1, x_2 + 2\varepsilon)$,

$$K_\varepsilon\left(\frac{x_1}{x}\right) = \frac{x^2}{x_1} \frac{d}{dx} \frac{\omega_\varepsilon(x) - \Gamma}{x^2}. \quad (60)$$

Thus, for $x \in (x_1, x_2 - \varepsilon)$ where $\omega_\varepsilon = \omega_*$,

$$K_\varepsilon\left(\frac{x_1}{x}\right) = \frac{x^2}{x_1} \frac{d}{dx} \frac{\omega_*(x) - \Gamma}{x^2} = \frac{x^2}{x_1} \frac{d}{dx} \int_{x_1/x}^1 K_*(\theta) d\theta = K_*\left(\frac{x_1}{x}\right), \quad (61)$$

or, equivalently,

$$K_\varepsilon(\theta) = K_*(\theta) \text{ for } \theta \in \left[\frac{x_1}{x_2 - \varepsilon}, 1 \right]. \quad (62)$$

Noting that

$$\mathbb{I}_{[x_1/(x_2+2\varepsilon), 1]}(\theta) K_\varepsilon(\theta) \rightarrow \mathbb{I}_{[x_1/x_2, 1]}(\theta) K_*(\theta) \quad (63a)$$

and

$$\mathbb{I}_{[x_1/(x_2+2\varepsilon), 1]}(\theta) G_\varepsilon(\theta) \rightarrow \mathbb{I}_{[x_1/x_2, 1]}(\theta) G_*(\theta) \quad (63b)$$

pointwise for a.e. θ as $\varepsilon \searrow 0$, we find that

$$\begin{aligned} \frac{\int_0^1 K_*(\theta) d\theta - \int_{x_1/(x_2+2\varepsilon)}^1 K_\varepsilon(\theta) d\theta}{\int_0^1 G_*(\theta) d\theta - \int_{x_1/(x_2+2\varepsilon)}^1 G_\varepsilon(\theta) d\theta} - \left(\frac{x_1}{x_2 + 2\varepsilon} \right)^2 \rightarrow \\ \frac{\int_0^1 K_*(\theta) d\theta - \int_{x_1/x_2}^1 K_*(\theta) d\theta}{\int_0^1 G_*(\theta) d\theta - \int_{x_1/x_2}^1 G_*(\theta) d\theta} - \frac{x_1^2}{x_2^2} = \frac{\int_0^{x_1/x_2} K_*(\theta) d\theta}{\int_0^{x_1/x_2} G_*(\theta) d\theta} - \frac{x_1^2}{x_2^2}. \end{aligned} \quad (64)$$

Recall that $0 \leq K_*(\theta) = G_*(\theta) \theta^2$, so that $K_*(\theta) \leq G_*(\theta) x_1^2/x_2^2$ on $[0, x_1/x_2]$. This implies that the right hand side of (64) is negative so that there exists $\varepsilon > 0$ such that

$$\frac{\int_0^1 K_*(\theta) d\theta - \int_{x_1/(x_2+2\varepsilon)}^1 K_\varepsilon(\theta) d\theta}{\int_0^1 G_*(\theta) d\theta - \int_{x_1/(x_2+2\varepsilon)}^1 G_\varepsilon(\theta) d\theta} < \left(\frac{x_1}{x_2 + 2\varepsilon} \right)^2. \quad (65)$$

In all of the following, we fix $\varepsilon > 0$ such that this inequality holds true, abbreviate $r = x_1/(x_2 + 2\varepsilon)$, and set $G(\theta) = G_\varepsilon(\theta)$ and $K(\theta) = K_\varepsilon(\theta)$ for $\theta \in [r, 1]$. We still need to define G and K on the interval $[0, r]$, which is done as follows.

Since $\int_0^r r^{-n} \theta^n d\theta \rightarrow 0$ as $n \rightarrow \infty$, we can choose n such that

$$r_*^2 \equiv \frac{\int_0^1 K_*(\theta) d\theta - \int_r^1 K_\varepsilon(\theta) d\theta - G_\varepsilon(r) \int_0^r r^{-n} \theta^{n+2} d\theta}{\int_0^1 G_*(\theta) d\theta - \int_r^1 G_\varepsilon(\theta) d\theta - G_\varepsilon(r) \int_0^r r^{-n} \theta^n d\theta} < r^2. \quad (66)$$

Define $b_1, b_2 \in C^3([0, r], \mathbb{R}_+)$ as the spline functions

$$b_1(\theta) = \mathbb{I}_{[0, r_*/2]}(\theta) \theta^4 (r_*/2 - \theta)^4, \quad (67a)$$

$$b_2(\theta) = \mathbb{I}_{[r_*/2, r_*]}(\theta) (r_* - \theta)^4 (\theta - r_*/2)^4. \quad (67b)$$

By the integral mean value theorem,

$$\frac{\int_0^r \theta^2 b_1(\theta) d\theta}{\int_0^r b_1(\theta) d\theta} = \frac{\int_0^{r_*} \theta^2 b_1(\theta) d\theta}{\int_0^{r_*} b_1(\theta) d\theta} < r_*^2 < \frac{\int_{r_*}^r \theta^2 b_2(\theta) d\theta}{\int_{r_*}^r b_2(\theta) d\theta} = \frac{\int_0^r \theta^2 b_2(\theta) d\theta}{\int_0^r b_2(\theta) d\theta}. \quad (68)$$

Now define $B_1, B_2: [0, 1] \rightarrow \mathbb{R}_+$ as

$$B_1(\lambda) = \lambda \int_0^r \theta^2 b_1(\theta) d\theta + (1 - \lambda) \int_0^r \theta^2 b_2(\theta) d\theta, \quad (69)$$

$$B_2(\lambda) = \lambda \int_0^r b_1(\theta) d\theta + (1 - \lambda) \int_0^r b_2(\theta) d\theta. \quad (70)$$

Clearly, $\frac{B_1(0)}{B_2(0)} > r_*^2$ and $\frac{B_1(1)}{B_2(1)} < r_*^2$. Hence, due to continuity with respect to λ , we can find $\lambda_* \in (0, 1)$ such that

$$\frac{B_1(\lambda_*)}{B_2(\lambda_*)} = r_*^2. \quad (71)$$

Finally, on the interval $[0, r)$, we define

$$K(\theta) = \frac{k_*}{B_1(\lambda_*)} (\lambda_* \theta^2 b_1(\theta) + (1 - \lambda_*) \theta^2 b_2(\theta)) + G_\varepsilon(r) \frac{\theta^{n+2}}{r^n}, \quad (72)$$

where k_* denotes the numerator of the fraction defining r_*^2 in (66). Further, we set $G(\theta) = K(\theta)/\theta^2$. Then K and G are continuous on $[0, 1]$, strictly positive on $(0, 1)$, and, by direct computation, satisfy

$$\int_0^1 K(\theta) d\theta = \int_0^1 K_*(\theta) d\theta \quad (73a)$$

and

$$\int_0^1 G(\theta) d\theta = \int_0^1 G_*(\theta) d\theta = \Gamma. \quad (73b)$$

Further, using (73a), (60), and the fact that $\omega_*(x_1) = 0$, we verify that

$$\omega_\varepsilon(x) = \begin{cases} \Gamma - x^2 \int_0^1 K(\theta) d\theta & \text{for } x \in [0, x_1), \\ \Gamma - x^2 \int_0^{x_1/x} K(\theta) d\theta & \text{for } x \in [x_1, x_2 + 2\varepsilon]. \end{cases} \quad (74)$$

on the entire interval $[0, x_2 + 2\varepsilon]$. Moreover, comparing (74) with (1) and noting that x_1 is the first and $x_2 + \varepsilon$ the second zero of ω_ε by construction, we see that ω_ε satisfies (1) at least on the interval $[0, x_2 + \varepsilon]$.

To complete the proof, we show that it is not possible to find a solution ω to (1) that extends to a non-degenerate solution past the interval $[0, x_2 + \varepsilon]$ on which $\omega = \omega_\varepsilon$. Assume that, on the contrary, such an extension exists. Then there exists a small interval $I = (x_2 + \varepsilon, x_2 + \varepsilon + \varepsilon_*)$ on which ω is either positive or negative. (Note that we must require that $\varepsilon_* < z_\varepsilon$, cf. (57) where z_ε is first introduced.) Suppose first that $\omega < 0$ on I . Then (74) continues to provide a solution for (1) on I , but ω_ε is positive there, a contradiction. Suppose then that $\omega > 0$ on I . Then, using (22) and (57), we express ω on the interval I as

$$\begin{aligned} \omega(x) &= \Gamma - x^2 \int_0^{\frac{x_1}{x}} K(\theta) d\theta - x^2 \int_{\frac{x_2+\varepsilon}{x}}^1 K(\theta) d\theta \\ &= \omega_\varepsilon(x) - x^2 \int_{\frac{x_2+\varepsilon}{x}}^1 K(\theta) d\theta \\ &= -\frac{1}{2} x^2 \int_{\frac{x_2+\varepsilon}{x}}^1 K_*(\theta) d\theta < 0. \end{aligned} \quad (75)$$

The last equality is due to (57) and (62) which is applicable for sufficiently small ε_* . Again, this contradicts the assumed sign of ω . Thus, we conclude that ω cannot be extended via formula (22) onto any right neighborhood of $x = x_2 + \varepsilon$. \square

6. EXTENDED SOLUTIONS FOR THE SIMPLIFIED HHMO-MODEL

So far, we have seen that precipitation band patterns as a sequence of intervals in which $\omega(x) > 0$, i.e. the reactant concentration exceeds the super-saturation threshold, must break down at a finite location x^* which is either an accumulation point given by Theorem 4, or until a point at which the solution degenerates after

a finite number of precipitation bands as in Theorem 9. In this section, we consider a more general notion of solution which is motivated by the construction of weak solutions to the full HHMO-model in [16].

Definition 12. A pair (ω, ρ) is an extended solution of the simplified HHMO-model if $\omega \in C([0, \infty))$,

$$\omega(x) = \Gamma - x^2 \int_0^1 K(\theta) \rho(x\theta) d\theta, \quad (76)$$

and ρ is a measurable function on $[0, \infty)$ taking values from the Heaviside graph, i.e.,

$$\rho(y) \in H(\omega(y)) = \begin{cases} 0 & \text{if } \omega(y) < 0, \\ [0, 1] & \text{if } \omega(y) = 0, \\ 1 & \text{otherwise.} \end{cases} \quad (77)$$

Theorem 13. If $K \in C([0, 1])$, then an extended solution to (76) exists.

Proof. Changing variables, we write (76) as

$$\omega(x) = \Gamma - x \int_0^x K\left(\frac{y}{x}\right) \rho(y) dy. \quad (78)$$

Now consider a family of mollified Heaviside functions $H_\varepsilon \in C^\infty(\mathbb{R}, [0, 1])$ parameterized by $\varepsilon > 0$ such that $H_\varepsilon(z) = 1$ for $z \geq \varepsilon$ and $H_\varepsilon(z) = 0$ for $z \leq -\varepsilon$. We claim that, for fixed $\varepsilon > 0$, the corresponding mollified equation

$$\omega_\varepsilon(x) = \Gamma - x \int_0^x K\left(\frac{y}{x}\right) H_\varepsilon(\omega_\varepsilon(y)) dy \quad (79)$$

has a solution $\omega_\varepsilon \in C([0, \infty))$. Indeed, suppose that ω_ε is already defined on some interval $[0, a]$, where a may be zero. We seek $\omega_\varepsilon \in C([a, a + \delta])$ which continuously extends ω_ε past $x = a$ as a fixed point of a map T from $C([a, a + \delta])$ endowed with the supremum norm into itself, defined by

$$T[\phi](x) = \Gamma - x \int_0^a K\left(\frac{y}{x}\right) H_\varepsilon(\omega_\varepsilon(y)) dy - x \int_a^x K\left(\frac{y}{x}\right) H_\varepsilon(\phi(y)) dy. \quad (80)$$

Since

$$\begin{aligned} |T[\phi](x) - T[\psi](x)| &= \left| x \int_a^x K\left(\frac{y}{x}\right) (H_\varepsilon(\psi(y)) - H_\varepsilon(\phi(y))) dy \right| \\ &\leq x \int_a^x \left| K\left(\frac{y}{x}\right) \right| \|H_\varepsilon(\phi) - H_\varepsilon(\psi)\|_{L^\infty} dy \\ &\leq x(x-a) \|K\|_{L^\infty} \|H'_\varepsilon\|_{L^\infty} \|\phi - \psi\|_{L^\infty}, \end{aligned} \quad (81)$$

T is a strict contraction for $\delta > 0$ small enough, hence has a unique fixed point. In addition, the maximal interval of existence of ω_ε is closed, as the right hand side of (79) is continuous, and open at the same time due to the preceding argument. Thus, a solution $\omega_\varepsilon \in C([0, \infty))$ exists (and is unique).

By direct inspection, for every fixed $b > 0$, the families $\{\omega_\varepsilon\}$ and $\{H_\varepsilon \circ \omega_\varepsilon\}$ are uniformly bounded in $C([0, b])$ endowed with the supremum norm. Moreover, $\{\omega_\varepsilon\}$ is equicontinuous. Indeed, for $y, z \in (0, b]$,

$$\left| \frac{\omega_{\varepsilon_i}(z) - \Gamma}{z} - \frac{\omega_{\varepsilon_i}(y) - \Gamma}{y} \right| \leq \int_0^{\max\{y, z\}} \left| K\left(\frac{\theta}{z}\right) - K\left(\frac{\theta}{y}\right) \right| d\theta, \quad (82)$$

where, by the dominated convergence theorem, the right hand side converges to zero as $z \rightarrow y$. Equicontinuity at $y = 0$ is obvious. Thus, by the Arzelá–Ascoli theorem, there exist a decreasing sequence $\varepsilon_i \rightarrow 0$ and a function $\omega \in C([0, b])$ such that $\omega_{\varepsilon_i} \rightarrow \omega$ in $C([0, b])$. Further, by the Banach–Alaoglu theorem, there exists $\rho \in L^\infty([0, b])$ such that, possibly passing to a subsequence, $H_{\varepsilon_i} \circ \omega_{\varepsilon_i} \rightharpoonup \rho$ weakly-* in L^∞ . This implies that ρ takes values a.e. from the interval $[0, 1]$ which contains the convex hull of the sequence. Passing to the limit in (79), we conclude that

$$\omega(x) = \Gamma - x \int_0^x K\left(\frac{y}{x}\right) \rho(y) dy. \quad (83)$$

Finally, we claim that $\rho(y) = 1$ whenever $\omega(y) > 0$. Indeed, fixing y such that $\omega(y) > 0$, equicontinuity of ω_ε implies that there exists a neighborhood of y on which ω_{ε_i} is eventually strictly positive. On this neighborhood, $H_{\varepsilon_i} \circ \omega_{\varepsilon_i}$ converges strongly to 1. A similar argument proves that $\rho(y) = 0$ whenever $\omega(y) < 0$.

So far, we have shown that (ω, ρ) satisfy (76) and (77) on $[0, b]$. To extend the interval of existence, we can iteratively restart the compactness argument on intervals $[0, nb]$ for $n \in \mathbb{N}$, passing to a subsequence each time. This proves existence of an extended solution on $[0, \infty)$. \square

Uniqueness of extended solutions is a much more delicate issue. In the following particular case, we can give a positive answer to the question of uniqueness.

Definition 14. *An extended solution (ω, ρ) to the simplified HHMO-model is regularly extended to an interval $[x^*, x^* + \varepsilon]$, where x^* is the point of breakdown in the sense of Theorem 4 or Theorem 9 and $\varepsilon > 0$, if $\omega \equiv 0$ on this interval.*

If (ω_1, ρ_1) and (ω_2, ρ_2) are pairs of regularly extended solutions to (76), then ω_1 and ω_2 coincide on $[0, x^*]$ by construction and on $[x^*, x^* + \varepsilon]$ by definition. Moreover, $\Delta\rho = \rho_1 - \rho_2 = 0$ on $[0, x^*]$. Thus, the question of uniqueness reduces to a statement on the non-existence of non-trivial solutions to the linear homogeneous integral equation

$$\int_0^1 K(\theta) \Delta\rho(x\theta) d\theta = 0 \quad (84)$$

for $x \in [0, x^* + \varepsilon]$. Due to properties (i)–(iii) of the kernel, the problem falls into the general class of weakly degenerate cordial Volterra integral equations. In [8], we answer this question in the affirmative.

While we believe that extended solutions are generically regularly extended, we cannot exclude the possibility that extended solutions develop a precipitation band pattern that accumulates at x^* from above. Thus, the general question of unique extendability remains open.

We conjecture that the question of uniqueness of extended solutions might be addressed by replacing Definition 12 by a formulation in terms of a mixed linear complementarity problem. To be concrete, write $\omega = \omega_+ - \omega_-$, where ω_+ is the positive part and ω_- the negative part of ω . Further, set $\sigma = 1 - \rho$ and define the vector functions

$$V = \begin{pmatrix} \sigma \\ \rho \end{pmatrix} \quad \text{and} \quad W = \begin{pmatrix} \omega_+ \\ \omega_- \end{pmatrix}. \quad (85)$$

Then we can formulate the extended solution as follows. Find $V \geq 0$, $W \geq 0$ such that

$$\mathcal{L}V + \mathcal{M}W + B = 0 \quad (86a)$$

subject to

$$\langle V, W \rangle = 0, \quad (86b)$$

where \mathcal{L} and \mathcal{M} are linear operators defined by

$$\mathcal{L}V = \begin{pmatrix} x^2 \int_0^1 K(\theta) \rho(x\theta) d\theta \\ \rho + \sigma \end{pmatrix}, \quad (86c)$$

$$\mathcal{M}W = \begin{pmatrix} \omega_+ - \omega_- \\ 0 \end{pmatrix}, \quad (86d)$$

and

$$B = \begin{pmatrix} \Gamma \\ -1 \end{pmatrix}. \quad (86e)$$

The angle brackets in (86b) denote the canonical inner product for vectors of $L^2((0, a))$ -functions,

$$\langle V, W \rangle = \int_0^a \omega_+(x) \sigma(x) dx + \int_0^a \omega_-(x) \rho(x) dx. \quad (87)$$

This formulation is known as a mixed linear complementarity problem. To make progress here, it is necessary to adapt Lions–Stampaccia theory [20] to the case of mixed complementarity problems; see, e.g., [4, 28], for different reformulations in a Sobolev space setting.

7. DISCUSSION

In this paper, we have identified a mechanism which leads to very rapid, i.e., finite-time equilibration of a dynamical system with memory that is “damped” via relay hysteresis. Past a certain point, a solution can only be continued in a generalized sense by “completing the relay”. We can assert existence and conditional uniqueness for the generalized solution, but full well-posedness remains open. Possible approaches are a reformulation of the concept of generalized solution in terms of a mixed linear complementarity problem as outlined above, or possibly a fixed point formulation using fractional integral operators. We believe that the integral equation (1) is a useful test bed for studying such approaches, with the hope to eventually transfer results to more general reaction-diffusion equations with relay hysteresis.

The detailed observed behavior is very much tied to property (i), the square-root degeneracy of the kernel K near $\theta = 1$. From the perspective of solving integral equations, this behavior is too degenerate for classical contraction mapping arguments as used by Volterra to apply, but it is sufficiently non-degenerate that strong results can still be proved, see the discussion in [8]. This degeneracy is associated with the scaling behavior of the heat kernel, so even when an exact reduction from a PDE to an integral equation, as is possible for the simplified HHMO-model, is not available, the associated phenomenology is expected to survive.

Let us finally remark on the connection of our models to the real-world Liesegang precipitation phenomenon. Our detailed results on the breakdown of patterns for the simplified model imply that we cannot expect the Keller–Rubinow family of models to provide a good literal description of Liesegang rings. However, the fact that, independent of the details of simplified vs. full dynamics, the models converge rapidly toward a steady-state which *only exists as a generalized solution*, we believe

that it might be possible to interpret fractional values of the precipitation function as a *precipitation density*. In this view, the model would provide a coarse-grained description of the phenomenon in the sense that the precise information about the location of the rings is lost, but the local average fraction of space covered by precipitation rings can still be asserted. If this suggested interpretation is valid, the explicit asymptotic profile detailed in Section 3 will provide a direct relationship between the parameters of the system and the *macroscopic* properties of the Liesegang pattern.

This point of view is different from that taken by Duley *et al.* [11]. As they numerically encountered a qualitatively similar breakdown of solutions in the full Keller–Rubinow model (the model without the fast reaction limit taken), they chose to modify the dynamics of the model by introducing a delay variable to smooth out the onset of precipitation. Their approach aims at a more physical description at the *microscopic* level, i.e., toward a model that can correctly represent the width and location of each individual Liesegang ring.

APPENDIX A. PROPERTIES OF THE SIMPLIFIED HHMO-KERNEL

In the following, we prove a collection of results on the asymptotic behavior of the kernel G as given in (16) which imply properties (i) and (ii). As a corollary, we obtain that G is integrable, i.e., that the integrals in (17) and (18) are finite. We have verified property (iii) numerically, which is easily done to machine accuracy. A proof seems feasible, but would be rather involved and tedious, and does not offer further insight into the problem.

We begin by observing that G is clearly continuous on $(-1, 0)$ and $(0, 1)$. Thus, we focus on the local asymptotics of G near $\theta = 1$, $\theta = -1$ and $\theta = 0$.

Lemma 15. $G(\theta) \sim \sqrt{\frac{2}{\pi}} \frac{u^*}{\alpha} \sqrt{1-\theta}$ as $\theta \rightarrow 1$.

Proof. Rearranging expression (16), applying the integral mean value theorem, and setting $\sigma^2 = \frac{4(\zeta^2 - \alpha^2 \theta^2)}{\alpha^4 \theta^2 (1-\theta)^2}$, we obtain

$$\begin{aligned} G(\theta) &= \frac{1}{\sqrt{\pi}} \int_{\alpha|\theta|}^{\alpha} \frac{\alpha\zeta}{\sqrt{\zeta^2 - \alpha^2 \theta^2}} \exp\left(-\frac{\alpha^4 \theta^2 (1-\theta)^2}{4(\zeta^2 - \alpha^2 \theta^2)}\right) \exp\left(-\frac{\alpha^2 (1-\theta)^2}{4}\right) \frac{\Phi(\zeta)}{\zeta^3} d\zeta \\ &= \frac{\Phi(\zeta_\theta)}{\sqrt{\pi} \zeta_\theta^3} \exp\left(-\frac{\alpha^2 (1-\theta)^2}{4}\right) \int_{\alpha|\theta|}^{\alpha} \frac{\alpha\zeta}{\sqrt{\zeta^2 - \alpha^2 \theta^2}} \exp\left(-\frac{\alpha^4 \theta^2 (1-\theta)^2}{4(\zeta^2 - \alpha^2 \theta^2)}\right) d\zeta \\ &= \frac{\Phi(\zeta_\theta) \alpha^3}{2\sqrt{\pi} \zeta_\theta^3} \exp\left(-\frac{\alpha^2 (1-\theta)^2}{4}\right) |\theta| (1-\theta) \int_0^{z(\theta)} \exp\left(-\frac{1}{\sigma^2}\right) d\sigma \end{aligned} \quad (88)$$

for some $\zeta_\theta \in [\alpha|\theta|, \alpha]$ and

$$z(\theta) = \frac{2}{\alpha|\theta|} \sqrt{\frac{1+\theta}{1-\theta}}. \quad (89)$$

When $\theta \rightarrow 1$, we have $z(\theta) \rightarrow \infty$. Then, as averages converge to asymptotic values,

$$\frac{1}{z(\theta)} \int_0^{z(\theta)} \exp\left(-\frac{1}{\sigma^2}\right) d\sigma \rightarrow 1. \quad (90)$$

For the prefactor in (88), we observe that

$$\lim_{\theta \rightarrow 1} \frac{\Phi(\zeta_\theta) \alpha^3}{2\sqrt{\pi} \zeta_\theta^3} \exp\left(-\frac{\alpha^2(1-\theta)^2}{4}\right) |\theta| \sqrt{1-\theta} z(\theta) = \sqrt{\frac{2}{\pi}} \frac{\Phi(\alpha)}{\alpha}. \quad (91)$$

Since $\Phi(\alpha) = u^*$, this altogether implies the claim. \square

Lemma 16. $G(\theta) \sim \sqrt{\frac{2}{\pi}} \frac{u^*}{\alpha^3} \exp\left(\frac{\alpha^2}{4}\right) (1+\theta)^{\frac{3}{2}} \exp\left(-\frac{\alpha^2}{2(1+\theta)}\right)$ as $\theta \rightarrow -1$.

Proof. First note that

$$\int_0^z \exp\left(-\frac{1}{\sigma^2}\right) d\sigma \sim \frac{z^3}{2} \exp\left(-\frac{1}{z^2}\right) \quad (92)$$

as $z \rightarrow 0$. Thus, in the limit $\theta \rightarrow -1$ with $z(\theta)$ given by (89),

$$\begin{aligned} \int_0^{z(\theta)} \exp\left(-\frac{1}{\sigma^2}\right) d\sigma &\sim \frac{4}{\alpha^3 |\theta|^3} \left(\frac{1+\theta}{1-\theta}\right)^{\frac{3}{2}} \exp\left(-\frac{\alpha^2 \theta^2}{4} \frac{1-\theta}{1+\theta}\right) \\ &\sim \frac{\sqrt{2}}{\alpha^3} (1+\theta)^{\frac{3}{2}} \exp\left(\frac{5}{4} \alpha^2\right) \exp\left(-\frac{\alpha^2}{2(1+\theta)}\right). \end{aligned} \quad (93)$$

Then, using expression (88) for $G(\theta)$ as in the proof of Lemma 15, noting that the limit of the prefactor can be obtained by direct substitution, and using (93), we obtain the claim. \square

Hence, G is continuous on $[-1, 0)$ and $(0, 1]$. We next determine the asymptotic behavior of G at $\theta = 0$ depending on κ . To simplify notation, we write

$$C_1 = \frac{u^*}{\alpha^\kappa M\left(\frac{\kappa}{2}, \kappa + \frac{1}{2}, -\frac{\alpha^2}{4}\right)}. \quad (94)$$

to denote the constant prefactor in the explicit expression (6) for Φ in the case $\eta < \alpha$.

Lemma 17. *When $\kappa > 2$, G extends to a continuous function on $[-1, 1]$ with*

$$G(0) = \frac{\alpha}{\sqrt{\pi}} \exp\left(-\frac{\alpha^2}{4}\right) \int_0^\alpha \frac{\Phi(\zeta)}{\zeta^3} d\zeta. \quad (95)$$

When $1 < \kappa < 2$, as $\theta \rightarrow 0$,

$$G(\theta) \sim |\theta|^{\kappa-2} C_1 \frac{\alpha^{\kappa-1}}{\sqrt{\pi}} \int_0^1 \exp\left(-\frac{\alpha^2}{4\sigma^2}\right) (1-\sigma^2)^{-\frac{\kappa}{2}} d\sigma. \quad (96)$$

Finally, when $\kappa = 2$, as $\theta \rightarrow 0$,

$$G(\theta) \sim -C_1 \frac{\alpha}{\sqrt{\pi}} \exp\left(-\frac{\alpha^2}{4}\right) \ln|\theta|. \quad (97)$$

Proof. We re-write (16) as

$$G(\theta) = \frac{\alpha}{\sqrt{\pi}} \int_0^\alpha f(\theta, \zeta) d\zeta \quad (98)$$

with

$$f(\theta, \zeta) = \mathbb{I}_{[\alpha|\theta|, \alpha]}(\zeta) \frac{1}{\sqrt{1-\frac{\alpha^2\theta^2}{\zeta^2}}} \exp\left(-\frac{\alpha^2(1-\theta)^2}{4\left(1-\frac{\alpha^2\theta^2}{\zeta^2}\right)}\right) \frac{\Phi(\zeta)}{\zeta^3}. \quad (99)$$

For $\theta < \frac{1}{2}$,

$$f(\theta, \zeta) \leq \sup_{z \in (0, \alpha^{-1})} \frac{1}{z} \exp\left(-\frac{\alpha^2}{16z^2}\right) \frac{\Phi(\zeta)}{\zeta^3}. \quad (100)$$

As the Kummer function in the expression for $\Phi(\zeta)$ from (6) limits to 1 as $\zeta \rightarrow 0$, this upper bound is integrable for $\kappa > 2$. The first case claimed in the lemma is thus a direct consequence of the dominated convergence theorem.

When $1 < \kappa \leq 2$, the integral in (98) is divergent as $\theta \rightarrow 0$. To determine its asymptotics, we apply the change of variables

$$\sigma^2 = 1 - \frac{\alpha^2 \theta^2}{\zeta^2} \quad (101)$$

and insert the explicit expression for Φ , so that

$$G(\theta) = C_1 \frac{\alpha}{\sqrt{\pi}} (\alpha\theta)^{\kappa-2} \int_0^{\sqrt{1-\theta^2}} g(\sigma; \sqrt{1-\theta^2}) (1-\sigma)^{-\frac{\kappa}{2}} d\sigma \quad (102)$$

with

$$g(\sigma; \xi) = \exp\left(-\frac{\alpha^2 (1 - \sqrt{1 - \xi^2})^2}{4\sigma^2}\right) M\left(\frac{\kappa}{2}, \kappa + \frac{1}{2}, -\frac{\alpha^2 (1 - \xi^2)}{4(1 - \sigma^2)}\right) (1 + \sigma)^{-\frac{\kappa}{2}}. \quad (103)$$

On the closed unit square, g is strictly positive and bounded.

When $1 < \kappa < 2$, the integrand in (102) is integrable on $[0, 1]$ so that once again the dominated convergence theorem applies, implying (96).

When $\kappa = 2$, we split the expression for g into two terms,

$$\begin{aligned} g(\sigma; \xi) &= \exp\left(-\frac{\alpha^2 (1 - \sqrt{1 - \xi^2})^2}{4\sigma^2}\right) \frac{1}{1 + \sigma} \\ &\quad - \frac{\alpha^2}{10} \exp\left(-\frac{\alpha^2 (1 - \sqrt{1 - \xi^2})^2}{4\sigma^2}\right) \frac{1 - \xi^2}{1 - \sigma^2} M\left(1, \frac{7}{2}, -\frac{\alpha^2 (1 - \xi^2)}{4(1 - \sigma^2)}\right) \frac{1}{1 + \sigma} \\ &\equiv T_1(\sigma; \xi) + \frac{1 - \xi}{1 - \sigma} T_2(\sigma; \xi). \end{aligned} \quad (104)$$

Clearly,

$$\int_0^\xi \frac{T_1(\sigma; \xi)}{1 - \sigma} d\sigma \sim -\frac{1}{2} \exp\left(-\frac{\alpha^2}{4}\right) \ln(1 - \xi) \sim -\exp\left(-\frac{\alpha^2}{4}\right) \ln|\theta|. \quad (105)$$

Moreover, using mean value theorem, for some $\sigma_\xi \in (0, \xi)$ we obtain

$$\int_0^\xi \frac{1 - \xi}{(1 - \sigma)^2} T_2(\sigma; \xi) d\sigma = (1 - \xi) T_2(\sigma_\xi; \xi) \int_0^\xi \frac{d\sigma}{(1 - \sigma)^2} = \xi T_2(\sigma_\xi; \xi). \quad (106)$$

As T_2 is bounded, the contribution from T_1 is asymptotically dominant as $\theta \rightarrow 0$. This implies (97). \square

Corollary 18. *The integrals in (17) and (18) are finite.*

Proof. We know that G is continuous on $[-1, 0)$ and $(0, 1]$. The asymptotic behavior of G near $\theta = 0$ is given by Lemma 17. We note that the functions $\ln|\theta|$ and $|\theta|^{\kappa-2}$ are integrable on any neighborhood of $\theta = 0$, therefore G and K are integrable on $[-1, 1]$. \square

Corollary 19. *The kernel K associated with equation (17) satisfies properties (i) and (ii).*

Proof. We can use Lemma 17 for all $\kappa > 1$ to obtain

$$K(0) = \lim_{\theta \searrow 0} K(\theta) = \lim_{\theta \searrow 0} \theta^2(G(\theta) + G(-\theta)) = 0. \quad (107)$$

Furthermore, we note that the same lemma implies

$$K'(0) = \lim_{\theta \searrow 0} \frac{K(\theta) - K(0)}{\theta - 0} = \lim_{\theta \searrow 0} \theta(G(\theta) + G(-\theta)) = 0. \quad (108)$$

This proves (i). Property (ii) is a direct consequence of Lemma 15. \square

APPENDIX B. NUMERICAL SCHEMES

We solve the full HHMO-model (10) and the simplified HHMO-model (11) in similarity variables, where the full model reads

$$s w_s - \eta w_\eta - 2 w_{\eta\eta} = \frac{2\gamma}{\eta^2} H(\alpha - \eta) \Phi - 2 s^2 p(\Phi + w), \quad (109a)$$

$$w_\eta(0, s) = 0 \quad \text{for } s \geq 0, \quad (109b)$$

$$w(\eta, s) \rightarrow 0 \quad \text{as } \eta \rightarrow \infty \text{ for } s \geq 0. \quad (109c)$$

Toward deriving a scheme, we *impose* a binary precipitation function so that $p(\eta, s) = 1$ if and only if $w(\eta', s') \geq u^* - \Phi(\eta')$ anywhere along the characteristic line $\eta s = \eta' s'$ with $s' \leq s$. Note that the change of variables maps the origin of the x - t plane onto the entire η -axis. Since $\sup_x |u(x, t) - \psi(x, t)|$ as $t \searrow 0$, we initialize with $u(\eta, 0) = \Psi(\eta)$, so that

$$w(\eta, 0) = \Psi(\eta) - \Phi(\eta) \quad \text{for } \eta \geq 0. \quad (109d)$$

The corresponding evolution equation for the simplified model is

$$s w_s - \eta w_\eta - 2 w_{\eta\eta} = \frac{2\gamma}{\eta^2} H(\alpha - \eta) \Phi - 2 s^2 p \Phi \quad (110)$$

where p is binary as before with $p(\eta, s) = 1$ if and only if $w(\eta', s') \geq u^* - \Phi(\alpha)$ for $\eta s = \alpha s'$ with $\eta \leq \alpha$. Boundary and initial condition are as for the full model.

The computational domain is taken as the finite interval $[0, 6\alpha]$, where the factor 6 is ensures sufficient accuracy for the essential part of the solution. Let N denote the grid cell at $\eta = \alpha$, $N_{\text{full}} = 6N$ the number of spatial mesh points, and $\Delta\eta = \alpha/N$ the spatial mesh size. Then the spatial mesh points are given by $\eta_i = i\Delta\eta$ for $i = 0, \dots, N_{\text{full}} - 1$. Similarly, the temporal mesh points are given by $s_j = j\Delta s$. We write w_i^j to denote the numerical approximation to $w(\eta_i, s_j)$, p_i^j to denote the numerical approximation to $p(\eta_i, s_j)$, and set $\Phi_i = \Phi(\eta_i)$. We use a first order upwind finite difference for the advection term and the standard second order finite difference approximation for the Laplacian. The boundary conditions are represented by $w_{-1}^j = w_0^j$ and $w_{6N+1}^j = 0$, respectively. In time, we use a simply first-order difference where the left hand side of the evolution equation is treated implicitly and the right hand side explicitly.

This leads to solving, at each time step, a system of linear equations $A^j w^j = b^{j-1}$ where A^j is the tridiagonal matrix with coefficients

$$a_{i,i}^j = j + i + 4/\Delta\eta^2 \quad \text{for } i = 0, \dots, N_{\text{full}} - 1, \quad (111a)$$

$$a_{i,i-1}^j = -2/\Delta\eta^2 \quad \text{for } i = 1, \dots, N_{\text{full}} - 1, \quad (111b)$$

$$a_{i,i+1}^j = -i - 2/\Delta\eta^2 \quad \text{for } i = 1, \dots, N_{\text{full}} - 2, \quad (111c)$$

$$a_{0,1}^j = -4/\Delta\eta^2, \quad (111d)$$

and b^{j-1} is the vector whose coefficients are given for the full model by

$$b_i^{j-1} = \frac{2\gamma}{\eta_i^2} H_{i \leq N} \Phi_i + j w_i^{j-1} - 2 s_j^2 p_i^{j-1} (\Phi_i + w_i^{j-1}) \quad (111e)$$

for $i = 1, \dots, N_{\text{full}} - 1$. For the simplified model, expression (111e) is modified to read

$$b_i^{j-1} = \frac{2\gamma}{\eta_i^2} H_{i \leq N} \Phi_i + j w_i^{j-1} - 2 s_j^2 p_i^{j-1} \Phi_i. \quad (112)$$

As the first term on the right of (109a) resp. (110) diverges for $\eta \searrow 0$ for $\gamma \in (0, 2)$, which true for the parameters used in this paper, we set $b_0^{j-1} = b_1^{j-1}$ in both cases; the resulting solution, however, is insensitive to the actual value used. This treatment is justified by observing that the resulting scheme is sufficiently accurate when applied to the analytically known self-similar solution Φ .

We use the following simple transport scheme for the precipitation function p . For both full and simplified model, and spatial indices $i < N$ corresponding to $\eta < \alpha$, we only need to transport the values of the precipitation function along the characteristic curves. We note that the characteristic curves define a map from the temporal interval $[0, s]$ at $\eta = \alpha$ to the spatial interval $[0, \alpha]$ at time $s = j\Delta s$. This map scales each grid cell by a factor N/j . We distinguish two sub-cases. For fixed time index $j \leq N$, a temporal cell is mapped onto at least one full spatial cell. Thus, we can use a simple backward lookup as follows. Let

$$\mathcal{J}(i; j) = \lfloor i \frac{j}{N} \rfloor \quad (113)$$

be the time index in the past that corresponds best to spatial index i . Then we set

$$p_i^j = p_N^{\mathcal{J}(i; j)}. \quad (114)$$

For a fixed time index $j > N$, we do a forward mapping, i.e., we define the inverse function to (113),

$$\mathcal{I}(k; j) = \lceil k \frac{N}{j} \rceil, \quad (115)$$

which represents the spatial index that the cell with past time index k and spatial index N has moved to, and set

$$p_i^j = \frac{N}{j} \sum_{\mathcal{I}(k; j)=i} p_N^k. \quad (116)$$

Note that this expression can yield values for p_i^j outside of the unit interval, which is not a problem as the integral over the entire interval is represented correctly. To implement this efficiently in code, we keep a running sum

$$P_j = \sum_{k=0}^j p_N^k \quad (117)$$

which can be updated incrementally and write

$$p_i^j = \frac{N}{j} (P_{\mathcal{J}(i+1;j)} - P_{\mathcal{J}(i;j)}). \quad (118)$$

This expression is equivalent to (116).

Finally, we need to determine the precipitation function p_i^j for $i \geq N$. For the simplified model, we set $p_N^j = 1$ whenever $w_N^j \geq u^* - \Phi_N$ and $p_N^j = 0$ otherwise; $p_i^j = 0$ for all $i > N$.

For the full model, we need to probe the entire region where $i \geq N$. In this region, whenever $w_i^j > u^* - \Phi_i$, the maximum principle for the continuum problem, see [9], implies that u exceeds the precipitation threshold on some curve contained in the region $\{s \leq s_j\}$ which connects the point (η_i, s_j) with the line $\eta = \alpha$. This implies that $p_k^j = 1$ for all $N \leq k \leq i$. Consequently, we only need to track the largest index I^j where precipitation takes place and set $p_k^j = 1$ for $k = N, \dots, I^j$. To do so, observe that precipitation takes place either when u exceeds the threshold, or when a cell lies on a characteristic curve where precipitation has taken place at the previous time step. This leads to the the expression

$$I^j = \max\{\max\{k: w_k^j > u^* - \Phi_k\}, \lfloor I^{j-1} (j-1)/j \rfloor\}, \quad (119)$$

which finalizes the description of the numerical scheme for the full model.

We remark that the scheme for the full model is almost equivalent to the scheme used in [9] which was formulated in terms of the concentration u . Here, to allow for switching between the full and the simplified model, it was necessary to formulate both schemes in terms of the difference variable $w = u - \phi$. Thus, the scheme given here differs from the scheme in [9] by terms that account for the difference between ϕ and its finite difference approximation.

ACKNOWLEDGMENTS

We thank Rein van der Hout for introducing us to the fast reaction limit of the Keller–Rubinow model, Arndt Scheel for interesting discussions on Liesegang rings and for bringing reference [10] to our attention, and an anonymous referee for helpful suggestions that improved the presentation of the paper. This work was funded through Deutsche Forschungsgemeinschaft (DFG, German Research Foundation) grant OL 155/5-1. Additional funding was received via the Collaborative Research Center TRR 181 “Energy Transfers in Atmosphere and Ocean”, also funded by the DFG under project number 274762653.

REFERENCES

- [1] M. ABRAMOWITZ AND I. A. STEGUN, eds., *Handbook of Mathematical Functions with Formulas, Graphs, and Mathematical Tables*, United States National Bureau of Standards, Washington, DC, USA, 1972.
- [2] T. AIKI AND J. KOPFOVÁ, *A mathematical model for bacterial growth described by a hysteresis operator*, in *Recent Advances in Nonlinear Analysis*, World Sci. Publ., Hackensack, NJ, 2008, pp. 1–10.
- [3] M. BROKATE AND J. SPREKELS, *Hysteresis and phase transitions*, vol. 121 of *Applied Mathematical Sciences*, Springer-Verlag, New York, 1996.
- [4] C. W. CRYER AND M. A. H. DEMPSTER, *Equivalence of linear complementarity problems and linear programs in vector lattice Hilbert spaces*, *SIAM J. Control Optim.*, 18 (1980), pp. 76–90.

- [5] M. CURRAN, P. GUREVICH, AND S. TIKHOMIROV, *Recent advance in reaction-diffusion equations with non-ideal relays*, in Control of Self-Organizing Nonlinear Systems, Underst. Complex Syst., Springer, 2016, pp. 211–234.
- [6] Z. DARBENAS, *Existence, uniqueness, and breakdown of solutions for models of chemical reactions with hysteresis*, PhD thesis, Jacobs University, 2018.
- [7] Z. DARBENAS AND M. OLIVER, *Conditional uniqueness of solutions to the Keller–Rubinow model for Liesegang rings in the fast reaction limit*. In preparation, 2018.
- [8] ———, *Uniqueness of solutions for weakly degenerate cordial Volterra integral equations*, J. Integral Equ. Appl., 31 (2019), pp. 307–327.
- [9] Z. DARBENAS, R. VAN DER HOUT, AND M. OLIVER, *Long-time asymptotics of solutions to the Keller–Rubinow model for Liesegang rings in the fast reaction limit*. Submitted for publication, 2018.
- [10] J. M. DULEY, A. C. FOWLER, I. R. MOYLES, AND S. B. G. O'BRIEN, *On the Keller–Rubinow model for Liesegang ring formation*, Proc. R. Soc. A, 473 (2017), p. 20170128.
- [11] ———, *Regularization of the Ostwald supersaturation model for Liesegang bands*, Proc. R. Soc. A, 475 (2019), p. 20190154.
- [12] P. GUREVICH, R. SHAMIN, AND S. TIKHOMIROV, *Reaction-diffusion equations with spatially distributed hysteresis*, SIAM J. Math. Anal., 45 (2013), pp. 1328–1355.
- [13] P. GUREVICH AND S. TIKHOMIROV, *Uniqueness of transverse solutions for reaction-diffusion equations with spatially distributed hysteresis*, Nonlinear Anal., 75 (2012), pp. 6610–6619.
- [14] H. K. HENISCH, *Crystals in Gels and Liesegang Rings*, Cambridge University Press, 1988.
- [15] D. HILHORST, R. VAN DER HOUT, M. MIMURA, AND I. OHNISHI, *Fast reaction limits and Liesegang bands*, in Free Boundary Problems. Theory and Applications, Basel: Birkhäuser, 2007, pp. 241–250.
- [16] ———, *A mathematical study of the one-dimensional Keller and Rubinow model for Liesegang bands*, J. Stat. Phys., 135 (2009), pp. 107–132.
- [17] J. B. KELLER AND S. I. RUBINOW, *Recurrent precipitation and Liesegang rings*, J. Chem. Phys., 74 (1981), pp. 5000–5007.
- [18] M. A. KRASNOSEL'SKIĬ AND A. V. POKROVSKIĬ, *Systems with hysteresis*, Springer-Verlag, Berlin, 1989. Translated from the Russian by Marek Niezgodka.
- [19] H.-J. KRUG AND H. BRANDTSTÄDTER, *Morphological characteristics of Liesegang rings and their simulations*, J. Phys. Chem. A, 103 (1999), pp. 7811–7820.
- [20] J.-L. LIONS AND G. STAMPACCHIA, *Variational inequalities*, Comm. Pure Appl. Math., 20 (1967), pp. 493–519.
- [21] I. D. MAYERGOYZ, *Mathematical models of hysteresis*, Springer-Verlag, New York, 1991.
- [22] A. MIELKE, F. THEIL, AND V. I. LEVITAS, *A variational formulation of rate-independent phase transformations using an extremum principle*, Arch. Ration. Mech. Anal., 162 (2002), pp. 137–177.
- [23] D. SMITH, *On Ostwald's supersaturation theory of rhythmic precipitation (Liesegang's rings)*, J. Chem. Phys., 81 (1984), pp. 3102–3115.
- [24] K. H. STERN, *The Liesegang phenomenon*, Chem. Rev., 54 (1954), pp. 79–99.
- [25] A. VISINTIN, *Evolution problems with hysteresis in the source term*, SIAM J. Math. Anal., 17 (1986), pp. 1113–1138.
- [26] A. VISINTIN, *Differential Models of Hysteresis*, vol. 111 of Applied Mathematical Sciences, Springer-Verlag, 1994.
- [27] ———, *Ten issues about hysteresis*, Acta Appl. Math., 132 (2014), pp. 635–647.
- [28] L.-C. ZENG, Q. H. ANSARI, AND J.-C. YAO, *Equivalence of generalized mixed complementarity and generalized mixed least element problems in ordered spaces*, Optimization, 58 (2009), pp. 63–76.

Email address, Z. Darbenas: z.darbenas@jacobs-university.de

Email address, M. Oliver: m.oliver@jacobs-university.de

(Z. Darbenas and M. Oliver) SCHOOL OF ENGINEERING AND SCIENCE, JACOBS UNIVERSITY, 28759 BREMEN, GERMANY